

1       **Testing Probabilistic Seismic Hazard Estimates Against Accelerometric**  
2                               **Data in two countries: France And Turkey**

3  
4       Hilal Tasan<sup>1</sup>, Céline Beauval<sup>1</sup>, Agnès Helmstetter<sup>1</sup>, Abdullah Sandikkaya<sup>2</sup>, and Philippe  
5   Guéguen<sup>1</sup>

6  
7  
8                               Geophysical Journal International  
9

10  
11       Accepted 2014 May 20. Received 2014 May 19; in original form 2013 October 22.  
12

13  
14  
15  
16       **Affiliations:**

17       <sup>1</sup> ISTERre, Université Grenoble Alpes, IRD, CNRS, OSUG, BP 53, F-38041 Grenoble, France

18       <sup>2</sup> METU, Department of Civil Engineering, Earthquake Engineering Research Center, Middle  
19       East Technical University, K6 Building, 06800 Ankara, Turkey

20  
21  
22       Corresponding authors:

23       Hilal Tasan (hilal.tasan@ujf-grenoble.fr)

24       Celine Beauval (celine.beauval@ujf-grenoble.fr)

25       Tel: +33 4 76 51 40 68 / +33 4 76 63 51 80

26       Fax: +33 4 76 63 52 52  
27

28  
29  
30       Abbreviated title : Testing PSH estimates against accelerometric data  
31  
32  
33  
34

## 35 **Summary**

36  
37 Probabilistic seismic hazard models (PSHM) are used for quantifying the seismic hazard at a  
38 site or a grid of sites. In the present study, a methodology is proposed to compare the  
39 distribution of the expected number of sites with exceedance with the observed number  
40 considering an acceleration threshold at a set of recording sites. The method is applied to  
41 France and Turkey. The French accelerometric database is checked to produce a reliable  
42 accelerometric dataset. In addition, we also used a synthetic dataset inferred from an  
43 instrumental catalogue combined with a ground-motion prediction equation. The results show  
44 that the MEDD2002 and AFPS2006 PSH models over-estimate the number of sites with  
45 exceedance for low acceleration levels (below  $40 \text{ cm.s}^{-2}$ ) or short return periods (smaller than  
46 50 yrs for AFPS2006 and 475 yrs for MEDD2002). For larger acceleration levels, there are  
47 few observations and none of the models is rejected. In Turkey, the SHARE hazard estimates  
48 can be tested against ground-motion levels of interest in earthquake engineering. As the  
49 completeness issue is crucial, the recorded data at each station is analysed to detect potential  
50 gaps in the recording. As most accelerometric stations are located on soil, accelerations at  
51 rock are estimated using a site-amplification model. Different minimum inter-site distances  
52 and station configurations are considered. The observed numbers of sites with exceedance are  
53 well within the bounds of the predicted distribution for accelerations between 103 and 397  
54  $\text{cm.s}^{-2}$ . For higher levels, both the observed number and the predicted percentile 2.5 are zero,  
55 and no conclusion can be drawn.

## 58 **1. INTRODUCTION**

59  
60 Probabilistic seismic hazard assessment is used for quantifying the seismic hazard on a site or  
61 on a grid of sites. Probabilistic seismic hazard maps are now the basis for establishing  
62 seismic building codes in most parts of the world. These maps provide at geographical  
63 locations the ground motions with given probabilities of being exceeded in a future time  
64 period. Typically for conventional buildings, probabilities of exceedance of 2% to 10% over  
65 a 50 years time window are taken into account, corresponding to return periods of 475 to  
66 2475 years. Several recent Opinion papers in Seismological Research Letters and Earthquake  
67 Spectra are encouraging hazard analysts to carry out tests (Stein et al. 2011, Stirling, 2012,

68 Iervolino, 2013). However, considering the observation time window in seismology (~100  
69 years at maximum for instrumental networks, and several centuries for historical data),  
70 testing at the return periods of interest in engineering seismology is a real challenge.  
71 Validation of the full probabilistic hazard curve with observations at a site is strictly  
72 impossible as several thousands of years of observation would be required (Beauval et al.  
73 2008). Nonetheless testing partially these models against observations is possible.

74

75 Since the first application of the Cornell-McGuire probabilistic method (Cornell 1968,  
76 McGuire 1976), some authors have proposed to compare hazard curves with observed  
77 intensity rates. For example in Papazachos et al. (1990), an intensity-magnitude relationship  
78 is used to generate the sequence of intensity observations at a site, as if an “observer” had  
79 been there continuously. This sequence is then converted into a recurrence curve at the site.  
80 The authors superimpose the “observed” rates with hazard curves evaluated in terms of  
81 intensities at a series of sites. More recently, Stirling and Petersen (2006) proposed a similar  
82 comparison of predictions with observations, with applications in New Zealand and in the  
83 United States, the main difference being that true macroseismic intensities were used.  
84 Intensities were converted into accelerations applying an equation. The authors discussed in  
85 detail the uncertainties that might influence the results and tried to understand the  
86 discrepancies. Another direction was explored in Mucciarelli et al. (2008), who reconstructed  
87 the intensity history at a site from observed intensities and calculated ones (based on  
88 epicentral information or neighbouring intensity observation). They chose not to include an  
89 intensity-acceleration conversion and compared probabilistic seismic hazard (PSH) and  
90 intensity-based recurrences through the ranking of hazard evaluated at many sites in Italy.  
91 Most of these studies acknowledged the difficulty of calculating observed rates from  
92 potentially short time windows. To counteract this limitation, they analysed the results  
93 considering all sites as a whole, a reasoning close to sampling in space.

94

95 At present, hazard curves are most often provided in terms of accelerations. Several authors  
96 proposed to compensate the short time periods of observations by sampling in space. Ward  
97 (1995) performed area-based probabilistic seismic hazard tests, based on a grid of sites where  
98 synthetic accelerations were predicted from an earthquake catalogue. More recently, Fujiwara  
99 et al. (2009) carried out a comparison between predictions and observations, taking  
100 advantage of the dense Japanese accelerometric network. Considering a ground-motion  
101 threshold, they summarized the hazard map in one number, the average probability of

102 exceedance over the grid of sites covering Japan, and compared this number with the  
103 percentage of accelerometric stations with exceedance (K-NET network). Using the recorded  
104 strong motions at the New Zealand network, Stirling and Gerstenberger (2010) calculated  
105 observed numbers of exceedance for two acceleration thresholds (100 and 200  $\text{cm.s}^{-2}$ ) and  
106 compared these numbers with the value predicted by the PSH analysis. Number of  
107 exceedances was compared first on a site-basis, then considering all sites at once. Albarello  
108 and D'Amico (2008) used a 30-yr time recording window of the Italian strong-motion  
109 network to test a PSH model against accelerations, considering all sites at once. The present  
110 study builds on these works, and develops a method for testing PSH estimates available at the  
111 sites of an accelerometric network, and for exploring the uncertainties of the method.

112  
113 The aim here is to test the final output of the probabilistic calculations, the hazard curve.  
114 Understanding the impact of the uncertainties of PSH components on the final output is not  
115 straightforward (e.g. Beauval and Scotti 2004), and we believe that the full PSH model needs  
116 to be tested. However, the comparison with observations can also be performed at the  
117 intermediary steps of the probabilistic calculations. Long-term seismicity models, predicting  
118 the frequencies, size, and locations of future earthquakes, can be tested against earthquake  
119 catalogues (e.g. Rhoades et al. 2002; Musson and Winter, 2011). Moreover, the ground-  
120 motion prediction equations (GMPEs) can be selected based on their fit to the available  
121 accelerometric data (e.g. Scherbaum et al. 2004). Such studies are underway in France; the  
122 difficulty here is to test ground-motion prediction equations developed from moderate-to-  
123 large events on low-magnitude datasets (see, e.g., Beauval et al. 2012). Testing the  
124 intermediate steps of the probabilistic calculation is complementary to testing the PSH  
125 output, but it should be underlined that conclusions from the former cannot be generalized to  
126 the later.

127  
128 In the first part of this article, we present the method developed to test probabilistic hazard  
129 estimates and explore uncertainties. The method is at first applied in metropolitan France, an  
130 example of low-to-moderate seismicity region, using datasets covering different observation  
131 time windows: ground-motion data recorded at the stations of the French Accelerometric  
132 Network (RAP), and synthetic ground motions predicted from an earthquake catalogue.  
133 Then, the same methodology is applied to a more active region, Turkey, using accelerometric  
134 data recorded by the Turkish strong-motion network.

135

136 **2. METHOD FOR TESTING PSH MODELS AGAINST OBSERVATIONS**

137

138 **2.1 Published methods**

139

140 As introduced by Ward (1995), the length of observation time windows can be compensated  
 141 by sampling in space. Thus, the consistency of a PSH model with observations is evaluated at  
 142 several locations at once. Following Albarello and D'Amico (2008), sites need to be distant  
 143 enough from each other. Acceleration occurrences must be independent from one site to the  
 144 other, and the ground-motion occurrences at the different sites are assumed to belong to the  
 145 same stochastic process. The acceleration thresholds with a given probability  $p$  of exceedance  
 146 in a given time window are inferred from the hazard curves at all sites. Albarello and  
 147 D'Amico (2008) considered only sites having the same lifetime (30 years, 68 sites). For each  
 148 site, either the threshold has been exceeded during the observation time window (success  
 149 with a probability  $p$  according to the PSH model), or there was no exceedance (probability  $1-$   
 150  $p$ ). The situation is comparable to a sequence of independent yes/no experiments. Therefore  
 151 the binomial distribution gives the expected number of sites with exceedances

152

153 
$$P(n) = \binom{N_s}{n} p^n (1-p)^{N_s-n} = \frac{N_s!}{n!(N_s-n)!} p^n (1-p)^{N_s-n} \quad (1)$$

154

155 where  $P(n)$  is the probability to observe  $n$  sites with exceedance out of the  $N_s$  sites,  $p$  is the  
 156 probability of an experiment resulting in a success. If the observed number corresponds to a  
 157 very low or very high probability (compared to a chosen confidence interval), the test  
 158 indicates that the model over- or under-predicts the observations.

159

160 Stirling and Gerstenberger (2010) proposed another approach, adapted to the New Zealand  
 161 accelerometric network where station lifetime varies a lot from one station to the other (from  
 162 6 to 44 years, 24 stations in 2009). The test aims at comparing the predicted and observed  
 163 number of exceedances, while Albarello and D'Amico (2008) compare the number of sites  
 164 with exceedance. At one site, for a given acceleration threshold  $g_0$ , a PSH model provides the  
 165 mean annual rate of exceedance  $\lambda_i$ . The mean expected number of exceedances is obtained by  
 166 multiplying the rate  $\lambda_i$  by the duration of the observation time window  $t_i$ . Again, accelerations  
 167 at a site are assumed to occur according to a stationary Poisson process. The Poisson

168 distribution, fully defined by its mean, provides the probability of observing a given number  
 169  $n$  of accelerations above the threshold  $g_0$ :

$$170 \quad P(n) = \frac{(\lambda_i t_i)^n e^{-\lambda_i t_i}}{n!} \quad (2)$$

171 where  $t_i$  is the time window at the site  $i$  with annual rate of exceedance  $\lambda_i$  given by the PSH  
 172 model. The authors defined the following simple statistical test: if the observed number falls  
 173 within the bounds of the distribution, defined by the percentiles 2.5 and 97.5%, the  
 174 observations are considered consistent with the model (model is not “rejected”). Stirling and  
 175 Gerstenberger (2010) first evaluated PSH models at individual sites and then gathering all  
 176 sites. They wrote p. 1408 “The summed analysis is conducted because the site-specific  
 177 comparisons often involve very few events and would yield meaningless results in many  
 178 cases”. The sites are far enough apart so that they can be considered independent in terms of  
 179 ground-motion exceedances. As the sum of independent Poisson processes constitutes a  
 180 Poisson process, the total number of exceedances observed over all sites is compared to the  
 181 distribution defined by the following mean:

$$182 \quad N_{total} = \sum_{sites} \lambda_i t_i \quad (3)$$

184  
 185 Stirling and Gerstenberger (2010) obtained different results when testing each site  
 186 individually and when considering all sites at once (Equation 3, threshold considered is 0.1g).  
 187 When testing each site individually, the model is not rejected at 22 out of 24 sites, i.e., the  
 188 observed number of exceedances is within the confidence interval of the Poisson distribution.  
 189 However, when testing the whole network at once, i.e. comparing the total observed and  
 190 predicted numbers of exceedances, the PSH model is rejected with 95% confidence, as it is  
 191 predicting fewer exceedances than have been observed in the historical period. This suggests  
 192 that testing the PSH model against the total number of exceedances is more meaningful than  
 193 individual tests.

194

## 195 **2.2 Method implemented in the present study**

196

197 The French and Turkish accelerometric network has been built progressively, since 1995 in  
 198 France and since 1973 in Turkey, and lifetime of stations varies from a few months to a few  
 199 decades. The test must be able to handle varying lifetimes to take advantage of the full

200 databases. A PSH calculation yields the probability that an acceleration level will be  
201 exceeded “at least once” over a time window. We prefer to focus on the number of sites with  
202 exceedance, rather than on the exact number of exceedances, although both studies are  
203 possible. In total, 62 sites in France are included in the analysis. The Monte Carlo method is  
204 used to sample the site-specific Poisson distributions (Equation 2), characterized by their  
205 means ( $\lambda_i t_i$ ), and generate numbers of acceleration exceedances for all sites (corresponding to  
206 time windows  $t_i$ ). One run yields one set of 62 numbers of exceedance. Sampling the Poisson  
207 distributions many times, many sets of numbers of exceedances are generated. All are  
208 compatible with the PSH model. For each run, we count the total number of sites with  
209 exceedance. Finally, 10.000 runs provide 10.000 total numbers of sites with at least one  
210 exceedance (out of 62), and a probability distribution can be built. This distribution describes  
211 the expected number of sites with exceedance, for a virtual network having the same number  
212 of stations as the accelerometric network, and the same lifetimes. This probability  
213 distribution has a shape very close to a binomial distribution. Note that in the case of  
214 Albarello and D’Amico (2008), where all sites have the same lifetime, this distribution is  
215 binomial and can be obtained analytically. In Fig. 1, as an example, the test is led considering  
216 5 RAP stations and a given acceleration threshold.

217  
218

### 219 **3. TESTING PSHA IN FRANCE**

220  
221

#### 222 **3.1. Building the accelerometric dataset**

223

224 In France, the first stations of the accelerometric network were installed in 1995 (French  
225 Accelerometric Network, RAP, Péquegnat et al. 2008). Since then, the number of stations has  
226 increased, reaching at present a total of 142 sites in Metropolitan France. Out of these 142  
227 sites, 69 are identified as ‘rock sites’ ( $V_{S30}$  shear-wave velocity at 30 m depth  $\geq 760$  m/s; see  
228 Régnier et al. (2010) and the information given on the RAP website). Most of these stations  
229 are located in the Pyrenees (19), Alps (33) and Lower Rhine Graben (5), regions with the  
230 highest seismic hazard in metropolitan France. The RAP stations are either in triggering  
231 mode or continuous recording stations. They consist of one three-component broadband  
232 accelerometric sensor (Kinematic episensors, except for some of the oldest stations having

233 Guralp CMG5). The database extends over 16 years, from June 1995 to July 2011, and  
234 contains 40431 records (horizontal two-components). To limit the size of the database, we  
235 selected only signals with Peak Ground Acceleration (PGA) higher than  $1 \text{ cm.s}^{-2}$ , whatever  
236 the magnitude of the earthquake, reducing the total number of records to 2207. Stations in  
237 buildings and boreholes are not used. Note that a few events recorded only on one horizontal  
238 component and on the vertical component are kept.

239  
240 After a careful check of the database, we identified several issues: bad association of records  
241 with responsible earthquake, shift of signal baselines, truncation of records, and low signal-  
242 to-noise ratio. For all signals, we checked the association with an earthquake by comparing  
243 the P-wave arrival time observed on the signal with the arrival time estimated from the  
244 earthquake location and origin time given in the RAP database. If the observed and estimated  
245 arrival times differed by more than 10 seconds, we looked for an explanation. Either the  
246 clock of the station was not correct or the record had not been associated with the right  
247 earthquake. For ten records, the associated earthquake was not correct and the appropriate  
248 one was extracted from the *Reness* earthquake catalogue (See “Data and Resources” section).  
249 For 54 signals, the shift was likely due to a clock problem of the station. Indeed, in most  
250 cases the time shift was a multiple of 60 seconds, as often observed for clock problems. Other  
251 issues encountered are shifts in the signal baselines and truncation of signals. Forty-two  
252 records contain a sudden shift in the baseline, which we corrected. Twenty-four records were  
253 clearly truncated after the occurrence of the peak amplitude, and thus the PGA could be  
254 estimated.

255  
256 The final dataset used for testing PSH models contains 701 two-component records at 47  
257 rock sites, corresponding to 551 earthquakes (Fig. 2). At the other 15 rock stations, no ground  
258 motion higher than  $1 \text{ cm.s}^{-2}$  occurred during their lifetime, these stations are nonetheless  
259 included in the analysis. To ensure independency of sites, stations located closer than 10 km  
260 to another rock station have been discarded (7 stations). In this case, we kept the station with  
261 the largest expected number of exceedances during the station lifetime. Twenty-eight stations  
262 have been recording between 5 to 10 years, and 29 of them have been recording between 10  
263 to 16 years. Three rock stations have recorded a PGA higher than  $100 \text{ cm.s}^{-2}$ , SAOF in the  
264 South-East Alps and PYBB/PYAD in the Pyrenees, whereas half of the stations recorded at  
265 maximum a PGA lower than  $10 \text{ cm.s}^{-2}$  (Fig. 2, Table S1 in Supplementary Files).

266



267 For our analysis, it is of primary importance to use a complete database, or at least to identify  
268 gaps in the recording. We identified potential gaps in a station recording by analysing the  
269 inter-event times (times between successive earthquakes) of the acceleration sequence, based  
270 on the raw RAP database (no threshold on the acceleration). Average inter-event times were  
271 calculated, and inter-event times larger than 10 times the mean were considered as gaps in the  
272 recording (station not functioning, Fig. 3). Station lifetimes were shortened accordingly  
273 (Table S1 in Supplementary Files). Another test can be applied to check the completeness of  
274 our database, using an earthquake catalogue and a GMPE. This test is however limited by the  
275 inherent variability of ground motions. Using the Cauzzi and Faccioli (2008) equation, which  
276 fits well the French dataset (Beauval et al. 2012), we looked for earthquakes in the Renass  
277 earthquake catalogue that should have produced a median acceleration larger than  $10 \text{ cm.s}^{-2}$   
278 at the stations considered. From 58 records, 8 were missing (2 at OGS1, 5 at PYCA, 1 at  
279 PYAT). Five of them occurred within previously identified gaps. For the three remaining  
280 earthquakes at PYAC and PYAT, we did not find an explanation for the missing record. The  
281 station seemed to be working correctly at the time of the earthquake, since it detected a few  
282 events in the preceding and following days. Even if the problem is mostly localized on two  
283 stations, this suggests that the fraction of missing records (after correcting from identified  
284 gaps in the monitoring) is around 5% (3/58).

285

286

### 287 **3.2 PSH models**

288

289 Two PSH models are considered in the present study. The MEDD2002 model has been  
290 derived for the official French seismic building code (Martin et al. 2002, Sollogoub et al.  
291 2007), which entered in 2010 into the French regulations. It is the first building code in  
292 France established from probabilistic seismic hazard methods following the Eurocode 8  
293 standards. The AFPS2006 model was developed later on (Martin and Secanell 2006),  
294 involving a different group of experts who were questioning some of the decisions taken in  
295 MEDD2002 and claiming that the hazard was too high. Both models rely on the same  
296 seismicity models. The main difference in AFPS2006 with respect to MEDD2002 is the  
297 treatment of magnitude conversions and the ground-motion prediction equations used. We  
298 refer to the reports (Martin et al. 2002, Sollogoub et al. 2007, Martin and Secanell 2006) for  
299 details on the models used and their implementation in a logic tree. We do not question any  
300 of the decisions taken in these studies. We simply use these models and test them, because

301 they are hazard references for France. The AFPS2006 study predicts hazard values that are  
302 always lower or equal to the values of MEDD2002 model (Sollogoub et al. 2007). The  
303 MEDD2002 results are only available for 4 return periods (100, 475, 975, 1975 years),  
304 whereas the AFPS2006 results are available for 10 return periods (5 to 10000 years). The  
305 stations locations usually do not fall on one of the grid nodes but in the middle of a cell  
306 ( $0.1^\circ \times 0.1^\circ$  for MEDD2002,  $0.2^\circ \times 0.2^\circ$  for AFPS2006), the hazard rate at the location of each  
307 station is given by the average values at the four cell's nodes.

308  
309 Minimum magnitudes used in the probabilistic calculations vary. In MEDD2002 study, the  
310 minimum magnitude is  $M_{L,LDG} = 4$  in local LDG magnitude (LDG, 2012), corresponding to a  
311 moment magnitude  $M_w$  around 3.5 (Drouet et al. 2010). The study uses  $M_{L,LDG}$  magnitude as  
312 a surrogate for  $M_S$ . In AFPS2006 study, the minimum magnitude varies with the GMPE used,  
313 between 2.5 ( $M_{L,LDG}$ ) and 5 ( $M_S$ ). In the present study, all accelerations recorded at the  
314 stations are taken into account, regardless of the magnitude of the earthquake. Uncertainties  
315 are present at all steps of the PSH calculation and the magnitudes contributing to PSHA  
316 cannot be related easily to the magnitudes of the accelerations recorded at the sites of the  
317 RAP. The original magnitudes of earthquake catalogues have been converted using equations  
318 established over restricted magnitude range or equivalence has been assumed between  
319 magnitude scales (Martin and Secanell 2006). Most GMPEs used in the PSH studies tested  
320 here are imported from other regions, they have not been tested against local data and it is not  
321 possible to prove that they are adapted to the full magnitude range nor that their variability is  
322 truly representative at the sites considered. Besides, the level of studies on site effects varies  
323 greatly from one site to the other, and the uncertainty on the assigned class is expected to be  
324 large.

325

326

### 327 ***3.3 Testing results at the RAP sites***

328

329 The PSH models provide median hazard curves as well as percentiles, deduced from the logic  
330 tree. Only the median hazard curve is considered here for a series of acceleration thresholds.  
331 The probability distributions for the number of sites with exceedance are obtained through  
332 Monte Carlo sampling based on 10,000 runs (Section 2.2). Tests show that 10,000 runs are  
333 large enough to get stable results. These distributions indicate the expected number of sites  
334 (out of the 62 rock sites) with at least one exceedance of the acceleration level over the

335 lifetime of the stations (449 years in total, corrected lifetimes, see Table S1 in the  
336 Supplementary Files).

337

338 The tests can be carried out only for the acceleration levels that have been considered in the  
339 PSHA calculations. The AFPS2006 study provides accelerations for 10 return periods  
340 between 5 and 10,000 years. Obviously, the accelerations corresponding to these return  
341 periods vary from one site to the other. We chose to lead the test for a fixed acceleration  
342 threshold, common to all sites. The useful range is defined by the maximum of minimum  
343 accelerations of hazard curves ( $23 \text{ cm.s}^{-2}$  for the return period 5 yrs), and by the minimum of  
344 maximum accelerations of hazard curves ( $130 \text{ cm.s}^{-2}$  for 10,000 yrs). The AFPS2006 model  
345 can thus be tested against observations in the range 23 to  $130 \text{ cm.s}^{-2}$ . The example in Fig. 4  
346 shows the results for  $23 \text{ cm.s}^{-2}$ . The sites with exceedance are highlighted on the map and the  
347 responsible earthquakes are indicated. The probability distribution has the shape of a  
348 binomial distribution, percentiles 2.5 and 97.5 correspond respectively to 9 and 21 sites with  
349 exceedance. The model predicts a higher number of sites with exceedance than the observed  
350 number. Note however that for acceleration thresholds higher or equal to  $40 \text{ cm.s}^{-2}$ , the test  
351 concludes on a consistency between predictions and observations, as will be discussed later  
352 on. The MEDD2002 study provides hazard results only for 4 return periods starting from 100  
353 years to 1975 yrs (there was no possibility to obtain the full hazard curves, C. Martin,  
354 personal communication). Considering the 62 RAP sites, there is no common acceleration  
355 range between the 62 sites. For this reason, the MEDD2002 model is tested for a fixed return  
356 period rather than a fixed acceleration threshold.

357

358 Results of the testing are displayed in Fig. 5. The test is carried out using the modified  
359 lifetimes of stations to account for gaps in the monitoring. For each acceleration threshold,  
360 the observed number of sites with exceedance is superimposed on the expected number of  
361 sites, a probability distribution characterized by its mean and percentiles 2.5 and 97.5%. For  
362 the model AFPS2006 (Fig. 5a), observations are consistent with the model, i.e. within the  
363 percentiles 2.5 and 97.5, for all acceleration thresholds above  $40 \text{ cm.s}^{-2}$ . For the two lowest  
364 levels tested ( $23$  and  $30 \text{ cm.s}^{-2}$ ), the observed number of sites with exceedance is much lower  
365 than predicted by the model. We tested AFPS2006 also at fixed return periods (Fig. 5b). The  
366 AFPS2006 model predicts more exceedances than observed at 20 years return period.  
367 Between 50 and 200 years, the model is consistent with the observed number of exceedances

368 (within the bounds). For 475 and 975 years, the test is not conclusive due to the lack of  
369 observed exceedances.

370

371 Results for MEDD2002 model are displayed for 100, 475 and 975 years (Fig. 5c). The  
372 observed number of sites with exceedance (1) is lower than the 2.5 percentile at 100 years (2  
373 exceedances) and the model is rejected. For 475 and 975 years, the model is not rejected,  
374 however there is no exceedance, and the 2.5 percentile is also zero. This is not surprising,  
375 since these return periods are large with respect to the total length of the observation time  
376 window. In such a case, very different models may be consistent with the observations. In  
377 order to obtain meaningful results, we need long enough time windows and/or a large enough  
378 number of sites so that the expected total number of exceedances is larger than zero.

379

380 Sampling the sites in space and testing the hazard estimates considering all sites at once  
381 require that acceleration occurrences are independent. To reduce the correlation between  
382 records, stations closer than 10km from each other have been excluded prior to the analysis  
383 (Section 3.1). Moreover, the list of earthquakes responsible for the threshold exceedances  
384 was systematically checked. When two records at two stations were produced by the same  
385 earthquake, we simply discarded the site with the lowest acceleration recorded. They are few  
386 cases where this situation occurs. Discarding sites to ensure independence of sites brings  
387 minor changes to the plots and does not change the conclusions (see Figs 4 and 5). At each  
388 station, the earthquakes responsible for the thresholds exceedances have also been analysed  
389 to avoid including accelerations related to clustered events. We looked for events located  
390 within 10km of each other and within a time window of 30 days. Following this criterion, all  
391 events taken into account in the testing are independent.

392

393

### 394 ***3.4 Enlarging the observation time windows: using accelerations inferred from an*** 395 ***earthquake catalogue***

396

#### 397 ***3.4.1. Methodology***

398

399 Recorded accelerations are the most exact data to compare with hazard curves, but  
400 observation time windows are short, with the longest station lifetime reaching 16 yrs. An  
401 alternative to recorded ground motions is to use “synthetic” accelerations inferred from an

402 earthquake catalogue. Earthquake catalogues provide information over longer time periods  
403 than accelerometric networks. The test can be performed following exactly the same  
404 methodology; the “only” difference is that accelerations at sites have been obtained thanks to  
405 a GMPE. This test has advantages with respect to the testing on records, such as longer time  
406 windows and a complete database over these windows. However a strong assumption has to  
407 be made regarding the choice of the GMPE.

408  
409 The LDG earthquake catalogue, from the Laboratoire de Détection Géophysique (LDG,  
410 2012) is the best candidate for this test. The first stations of the LDG network were installed  
411 in 1962. The catalogue consists of 15993 earthquakes with magnitudes from 2.5 to 5.9  
412 ( $M_{L\_LDG}$ ), and spatial extension  $41^\circ$  to  $52^\circ$  in latitude and  $-6^\circ$  to  $10^\circ$  in longitude. For the  
413 purpose of this study, aftershocks should be removed from the catalogue because the PSH  
414 model is not taking into account aftershocks and is predicting Poissonian rates. Therefore, the  
415 LDG catalogue is declustered using the Reasenberg declustering algorithm (Reasenberg  
416 1985). Some 4776 events are identified as clustered events and removed from the catalogue.  
417 Then, the completeness is evaluated by plotting the cumulative number of earthquakes versus  
418 time. The catalogue is considered complete for magnitudes  $M_{L\_LDG} \geq 2.5$  from 1978 on.  
419 Thirty-four years are available for the test.

420  
421 The synthetic accelerometric history at a site is constructed using the earthquake catalogue  
422 coupled with a ground-motion prediction equation. For all earthquakes in the catalogue, the  
423 corresponding acceleration is calculated at the site. A GMPE adapted to the region under  
424 study must be selected. The variability  $\sigma$  of ground motions must be taken into account (e.g.  
425 Strasser et al. 2009). For one magnitude and one source-to-site distance, the GMPE provides  
426 a Gaussian probability distribution for the expected ground motion at the site. Therefore,  
427 through Monte Carlo sampling, many accelerometric histories are generated by sampling the  
428 Gaussian probability distributions. Instead of producing one set of accelerometric histories  
429 (median values), 10,000 sequences are generated, and the distribution for the “observed”  
430 number of sites with exceedance is obtained. Note that the Gaussian distribution must be  
431 sampled within meaningful limits. PSHA studies are usually calculating probabilities of  
432 exceedance of ground-motions truncating the Gaussian distribution at  $\pm 2\sigma$  or  $\pm 3\sigma$ . In our  
433 tests, a higher level of truncation allows higher accelerations and might have an impact on the  
434 “observed” number of sites with at least one exceedance. This number might be larger when

435 truncating at  $\pm 3\sigma$  than when truncating at  $\pm 2\sigma$ . The tests are performed for both truncation  
436 levels, however the results show that the truncation level has a minor impact on the results.

437

### 438 3.4.2. Selection of the GMPE

439

440 Two GMPE models have been identified as best fitting the French accelerometric data in  
441 Beauval et al. (2012), Cauzzi and Faccioli (2008, CF2008) developed from crustal Japanese  
442 data (80% of the dataset), and Akkar and Bommer (2010, AB2010) developed from data  
443 recorded in Europe and the Middle East. The dataset tested in Beauval et al. (2012) was made  
444 of earthquakes with  $M_w$  ranging between 3.8 and 4.5, and epicentral distances up to 300km.  
445 Here we check the fit of these equations with the actual dataset, going down to lower  
446 magnitudes and including only accelerations higher than  $1 \text{ cm.s}^{-2}$ . CF2008 and AB2010  
447 model have been developed from data with  $M_w \geq 5$ , both models are therefore applied below  
448 their magnitude validity limits. We refer to Beauval et al. (2012) for a detailed discussion on  
449 the regional dependence of GMPEs and on the use of GMPEs outside their validity limits.  
450 Another model is tested, which could be better adapted to a lower magnitude dataset, the  
451 Atkinson and Boore (2011) equation developed from earthquakes with  $M_w \geq 3.0$  recorded in  
452 western North American (update of the Boore and Atkinson (2008) equation extended  
453 towards lower magnitudes). All records available at the 54 RAP stations classified as 'rock',  
454 with PGA higher than  $1 \text{ cm.s}^{-2}$ , are taken into account (class A, 746 records, 578 events). For  
455 around 160 events, an  $M_w$  has been calculated by Drouet et al. (2010); for the other events,  
456 magnitudes  $M_{L\_LDG}$  are converted to  $M_w$  using the equation of Drouet et al. (2010).

457

458 Histograms of the residuals are superimposed on the standard normal distribution  
459 representing each GMPE model (Fig. 6, first column). The best fitting model is Cauzzi and  
460 Faccioli (2008), since the mean of the residuals is close to 0 and the standard deviation close  
461 to 1.0. Akkar and Bommer (2010) model also provides a good fit to the data, with a mean  
462 slightly shifted towards higher values (slight under-prediction of the model) and a variability  
463 slightly larger than the dispersion predicted by the model. Atkinson and Boore (2011)  
464 predicts a much lower variability in the dataset than is observed, although providing a rather  
465 good fit for the mean. The residuals are plotted versus  $M_w$  and versus source-site distances to  
466 highlight potential trends (Fig. 6). In the case of the CF2008 model, mean of residuals are  
467 rather stable with magnitude (no specific trend, and contained within  $\pm\sigma$ ), and rather stable  
468 also with source-to-site distance. These remarks also hold for the AB2010 model, except that

469 the residuals are more dispersed. In the case of the AB2011 model, a strong trend is observed  
470 for residuals depending on the distance, implying that the attenuation with distance as  
471 modelled in AB2011 does not reproduce observed attenuation of ground motions in France.

472  
473 Based on these results, Cauzzi and Faccioli (2008) is confirmed as the best-fitting model and  
474 selected for the present study. The model has a large  $\sigma$  value, which fits well the rather large  
475 dispersion in the French dataset. This large dispersion is both natural (true variability of the  
476 ground motions) and due to uncertainties in the metadata (magnitude estimates, source  
477 location, site classification, etc.). Note that the sigma predicted by the CF2008 model is much  
478 larger than the sigma predicted by the Atkinson and Boore (2011) model (CF2008: 0.344,  
479 AB2011: 0.246,  $\log_{10}$  units, for the PGA). The standard deviations in Atkinson and Boore  
480 (2011) have not been adjusted to lower magnitudes and are representative of larger events  
481 ( $M_w > 5.5$ ), on purpose (see their paper).

### 483 *3.4.3. Testing PSHM at the sites of the RAP stations with synthetic data*

484  
485 The test is first carried out exactly as in Section 3.3. At the 62 sites, locations of RAP  
486 stations, the synthetic time histories are now 34 years long. Assuming that the accelerations  
487 belong to the same stochastic process, and sampling the sites in space, leads to a virtual site  
488 with a total observation time window equal to 2018 years. This time window is more than  
489 four times longer than the total observation time window stacking the true-recorded periods  
490 at the same sites (449 years). The probability distribution for the observed number of  
491 exceedance is obtained by combining earthquakes in the LDG catalogue with the CF2008  
492 GMPE, which is sampled in the range  $\pm 3\sigma$ .

493  
494 The results obtained for the AFPS2006 and for the MEDD2002 models (Figs 7a and 7b) are  
495 very similar to those obtained from real data (Figs 5a and 5c). The predictions of the  
496 AFPS2006 model fit the synthetic observations above  $40 \text{ cm.s}^{-2}$ . For the lowest acceleration  
497 levels ( $23\text{-}30 \text{ cm.s}^{-2}$ ) the model overestimates the observations, the mean of the synthetic  
498 distribution is lower than the percentile 2.5 of the predicted distribution. The comparison with  
499 the predictions based on MEDD2002 model is once again difficult as the return periods tested  
500 are long and result in few observations at 475 and 975 yrs (Fig. 7b). At 100 yrs, the model  
501 over-estimates the observations (like in the real case, Fig. 5c). At 475 and 975 years, the

502 mean of observations is within the bounds, however both 2.5 percentiles correspond to 0 site  
503 with exceedance. Results obtained from sampling between the CF2008 Gaussian PDF  
504 between  $\pm 2\sigma$  are slightly different, with slightly lower numbers of sites with exceedance, but  
505 the main features remain identical (Figs. 7c and 7d). Moreover, independency of sites is  
506 required in these tests. When 10000 synthetic datasets are generated, the independency of  
507 exceedances at 62 stations is controlled by checking the earthquakes causing exceedance. If  
508 two ground-motion exceedances at two different stations are produced by the same  
509 earthquake, these stations are considered as dependent and the observed number of sites with  
510 exceedance is decreased. Removing correlated accelerations has no influence on the results  
511 (Fig. 7).

512  
513 The LDG catalogue consists of earthquakes with  $M_{L,LDG} \geq 2.5$ . While generating synthetic  
514 accelerations histories, all earthquakes are used. In order to understand the effect of this  
515 magnitude threshold on the results, the tests on the AFPS2006 model are performed again  
516 increasing the minimum bound for magnitude of earthquakes. Results based on the LDG  
517 catalogue taking into account  $M_{L,LDG} \geq 3.5$  are displayed in Fig. 8. The results still highlight a  
518 consistency between predictions and observations for the upper acceleration range (above 60  
519  $\text{cm.s}^{-2}$ ), and an over-prediction of the model for lower accelerations. However, the model is  
520 now strongly over-predicting the number of sites with exceedance, the mean of observations  
521 is much lower than the predicted 2.5 percentile. In the synthetic tests, the magnitudes  
522 between 2.5 and 3.5 are contributing largely in the range 23-50  $\text{cm.s}^{-2}$ .

523

#### 524 *3.4.4 Stability in time*

525 The PSH models have been tested against the RAP accelerometric data recorded between  
526 1995 and 2011. One question posed is whether this time period is representative for the  
527 acceleration levels involved, or in other words, if the observed numbers of sites with  
528 exceedance are stable when considering different observation time windows. Using the LDG  
529 catalogue, this hypothesis can be checked, as the catalogue provides 34 years of synthetic  
530 observations at each RAP station. The LDG catalogue is divided into five sliding time  
531 periods of 16 years (from 1978 to 2011). Each period is extending over the same duration as  
532 the RAP network. However, some stations of the network covers 16 years, while others cover  
533 much shorter durations. Within each period, the accelerometric history at each station is  
534 generated using a sub-division of the period, equal to the observation time available at that



535 station. Again, the Cauzzi and Faccioli (2008) equation is used to build the synthetic  
536 accelerometric histories. The same testing procedure is applied to the five time periods (Fig.  
537 9). For each period, the synthetic distribution for the “observed” number of sites with at least  
538 one exceedance is superimposed on the predicted distribution (AFPS2006 model). The results  
539 are stable from one period to the other. Below 40-60  $\text{cm.s}^{-2}$  predicted means are always lower  
540 than “observed” means, similarly to the results displayed in the real case (Fig. 5a) and when  
541 using 34 yrs of synthetic data (Fig. 7a). Above these levels, both the means and the  
542 percentiles approximately fit, for the five time periods. These results based on a sampling  
543 over France tend to show that 16 years of data is a representative period for the acceleration  
544 levels considered in the testing.

545

546

547

#### 548 **4. TESTING PSHA IN TURKEY**

549

550 A similar study is led in Turkey, a region of much higher seismic activity, where hazard  
551 estimates can be tested over a higher acceleration range, of greater interest in earthquake  
552 engineering. The probabilistic seismic hazard results obtained during the SHARE project are  
553 considered (Giardini et al. 2013, [www.share-eu.org](http://www.share-eu.org)). Hazard estimates corresponding to the  
554 logic-tree means are tested against accelerometric data. The minimum magnitude used in the  
555 probabilistic calculation is  $M_w$  4.5. For predicting ground motions, SHARE selected four  
556 GMPEs (Delavaud et al. 2012, respectively with weights 0.35, 0.35, 0.1, 0.2): Akkar and  
557 Bommer (2010) based on data from Europe and the Middle East; Cauzzi and Faccioli (2008)  
558 developed for Italy and based mostly on Japanese data (80% of the generating dataset); Zhao  
559 et al. (2006) based on Japanese data; Chiou and Youngs (2008) based mostly on Western  
560 North American data.

561

562

##### 563 ***4.1 Building the accelerometric dataset***

564

565 In Turkey, the first strong-motion instruments were installed in 1973 (Kinematics SMA-1  
566 type), and the first significant earthquake recorded in 1976 (Denizli earthquake, 19/08/1976).  
567 Since then, a nationwide strong-motion network has been established, operated by the  
568 Earthquake Research Department (ERD) of the General Directorate of Disaster Affairs

569 (GDDA). At the beginning of 2009, the total number of strong motion stations in the national  
570 network was 327, all equipped with digital recorders. In 2005, a project entitled  
571 « Compilation of Turkish strong motion network according to the international standards »  
572 was launched by ERD-GDDA and Middle East Technical University. The Turkish National  
573 strong-motion Project (T-NSMP) led to the building of the new Turkish strong-motion  
574 database (<http://kyh.deprem.gov.tr/>; Akkar et al. 2010). Accelerometric data from the national  
575 network stations of Turkey was compiled, processed and archived using state-of-art  
576 techniques. The site characterization of 241 (out of 327) strong-motion stations were  
577 improved, either by reassessing the existing shear-wave velocity profiles and soil column  
578 lithology information, or by utilizing invasive or non-invasive site exploration techniques to  
579 compute  $V_{S30}$  and other relevant parameters (Yılmaz et al. 2008, Akkar et al. 2010,  
580 Sandikkaya et al. 2010). The majority of the events in the database are shallow crustal  
581 earthquakes (depths less than 15 km) associated with the transform North and East Anatolian  
582 faults that run in the west–east and southwest–northeast orientations across the country. The  
583 few earthquakes with depths exceeding 40 km have occurred mostly in the southwest and  
584 eastern parts of Turkey falling on the Hellenic Arc and the Bitlis-Zagros Suture Zone,  
585 respectively (Bozkurt 2001). Most events in the database are for earthquakes with strike-slip  
586 and normal faulting.

587  
588 The main source of our accelerometric dataset is the Reference Database for Seismic Ground-  
589 Motion in Europe (RESORCE, Akkar et al. 2014). RESORCE is a single integrated  
590 accelerometric databank for the broader European area, consisting of earthquake and station  
591 metadata information, and accelerometric data. The Turkish component of RESORCE relies  
592 strongly on the T-NSMP database, covering the time window between 1976 and 2011, and  
593 including ground motions from magnitudes 2.8 to 7.6 (Mw). In RESORCE, the waveforms of  
594 raw accelerometric data were visually inspected one by one in terms of waveform quality and  
595 frequency content to implement a well-established data processing technique into the entire  
596 strong-motion databank (see Akkar et al. 2014 for details on the band-pass filtering and post-  
597 processing scheme). The primary parameter used for strong-motion site characterization is  
598  $V_{S30}$ . Source-to-site distance measures are provided (e.g. Joyner and Boore distance  $R_{JB}$ ).

599  
600 In the present study, we focus on accelerations greater than or equal to  $50 \text{ cm.s}^{-2}$ , recorded at  
601 stations with known  $V_{S30}$ . Fifty-six records with a geometrical mean higher or equal to 50

602  $\text{cm.s}^{-2}$  are extracted from RESORCE. As completeness is a key aspect for testing PSHA  
603 against observations, we must go back to the raw data from the Turkish Strong Motion  
604 network (TR-NSMN, <http://kyh.deprem.gov.tr>) to look for recordings that have been  
605 discarded, and to extend the time window to March 2013 (13/03/2013). Fifty-nine raw  
606 records, with a PGA greater than or equal to  $50 \text{ cm.s}^{-2}$  on at least 1 horizontal component are  
607 extracted from the database (no condition on the magnitude). Applying the same signal  
608 processing as performed in RESORCE (Akkar et al. 2014), 44 recordings are left with a  
609 geometrical mean greater than or equal to  $50 \text{ cm.s}^{-2}$ . Gathering the 56 records from  
610 RESORCE and these 44 records, the dataset consists of 100 records. In total, 291 Turkish  
611 stations could be used in the testing, with a  $V_{S30}$  provided either by RESORCE (235 stations)  
612 or by the TR-NSMN (56 stations).

613

614 The SHARE probabilistic seismic hazard curves are calculated for rock sites ( $V_{S30}$  800 m/s),  
615 whereas less than 6% of the Turkish stations are actually located at rock. Using a subset of  
616 the SHARE strong-motion database (Yenier et al. 2010), Sandikkaya et al. (2013) developed  
617 a site-amplification function that considers both linear and nonlinear soil effects. This site-  
618 amplification model was developed with the data from shallow crustal earthquakes and  
619 Turkey is one of the most contributing countries in the dataset. It provides the logarithm of  
620 the amplification as a function of  $V_{S30}$  and of the acceleration at rock (750 m/s), with  
621 coefficients depending on the spectral period (Eq. 5 and Table 3 in Sandikkaya et al. 2013).  
622 For a soil site, the amplification corresponds to the PGA recorded ( $\text{PGA}_{\text{SOIL}}$ ) divided by the  
623 PGA at rock ( $\text{PGA}_{\text{ROCK}}$ ).  $\text{PGA}_{\text{ROCK}}$  at all accelerometric stations are therefore obtained by  
624 fixing a first starting value for  $\text{PGA}_{\text{ROCK}}$  (using a ground-motion prediction equation at rock),  
625 then estimating the amplification and the corresponding value on soil, and after several  
626 iterations the  $\text{PGA}_{\text{ROCK}}$  yielding the exact  $\text{PGA}_{\text{SOIL}}$ , given the predicted amplification, is  
627 finally obtained. After conversion to a PGA corresponding to 750 m/s, 69 records are still  
628 higher or equal to  $50 \text{ cm.s}^{-2}$ .

629

630 For testing PSHA against observations, completeness is a key aspect, operating lifetime of  
631 stations must be known, as well as the periods when the stations were out of order.  
632 Unfortunately, this information is not available for most of Turkish stations. A quick look at  
633 the data shows that some stations have been operating only a few months, sometimes with  
634 years apart. The gaps in the data can only be estimated from the recording histories. Given

635 the uncertainty on the detection of these gaps, two methods are proposed here which provide  
636 two sets of complete time windows. These methods make use of all the (raw) data recorded at  
637 the stations, without any threshold amplitude. At 87 stations (out of 291), less than 2 records  
638 are available, and nothing can be inferred from this data about their operating lifetime. These  
639 stations are discarded. Applying the methods for detecting gaps (Section 4.2), 15 stations are  
640 left with observation time window equal to zero. Therefore, our dataset is finally made of 189  
641 stations, with 30 stations which recorded 56 PGA higher or equal to  $50 \text{ cm.s}^{-2}$  (Fig. 10,  
642 Tables S2 and S3 in the Supplementary Files).

643

644

## 645 ***4.2 Detecting gaps in the data***

646

### 647 *4.2.1 Technique based on average inter-event times*

648

649 In the first method, the gaps in the (raw) data are detected based on the average inter-event  
650 time (as in Section 3.1 for French stations). The Turkish dataset contains a significant amount  
651 of clustered events. The average inter-event time is calculated taking into account only  
652 independent accelerations produced by mainshocks. All inter-event times longer than 10  
653 times the average are considered as gaps. The algorithm from Reasenber (1985) is applied  
654 on the earthquake catalogue (with the following parameters, distance factor=15, minimum  
655 look-ahead time=10 days, maximum look-ahead time=20 days). Around 70% of the  
656 earthquakes are identified as foreshocks or aftershocks. At each station, the average inter-  
657 event time is calculated from the accelerations generated by mainshocks, and the time periods  
658 identified as gaps are retrieved from the lifetime of the station. The average inter-event time  
659 including a gap is over-estimated, thus this operation is repeated until no more gap is  
660 identified. Note that at all stations, we check that the gaps identified do not contain any  
661 acceleration from foreshock or aftershock events (in a very few cases it happens, and the gap  
662 is shortened). Fig. 11 displays the results for two stations. At station 5902 a gap is identified  
663 and the lifetime of the station is reduced from 18 to 13 years. At station 1608 no gap is  
664 identified and the station lifetime is not modified. The results show that the method is quite  
665 efficient for obvious long gaps in the data, nonetheless the choice of the factor 10 is rather  
666 arbitrary, and the method is not able to identify shorter gaps.

667

### 668 *4.2.2 Technique based on ground motion predictions*

669

670 In the second method, gaps in the data are identified thanks to synthetic accelerations,  
671 obtained by coupling a ground-motion prediction equation with the earthquake catalogue  
672 used in the SHARE project for Turkey (instrumental part, the SHARE Catalogue for Central  
673 and Eastern Turkey complementing the SHARE European Earthquake Catalogue, available at  
674 <http://www.emidius.eu/SHEEC/>, Grünthal et al. 2013, Sesetyan et al. 2013). As this  
675 European catalogue stops in 2006, the earthquake catalogue from B.Ü. KOERI National  
676 Earthquake Monitoring Center is used for the period 2006-2013 ([www.koeri.boun.edu.tr](http://www.koeri.boun.edu.tr)).  
677 The Akkar and Çağnan (2010) GMPE, developed from Turkish accelerometric data, is  
678 selected. At each station, for all earthquakes in the catalogue the median acceleration  
679 predicted at the site is calculated, and the synthetic history of accelerations is obtained.  
680 Details on the determination of the parameters required for predicting accelerations are given  
681 in Appendix A. The acceleration is calculated taking into account the  $V_{S30}$  value of the  
682 station. A quick analysis of the raw data shows that when a station was operating, the  
683 detection threshold was always lower than  $10 \text{ cm.s}^{-2}$ . Here gaps are identified each time one  
684 or more acceleration higher or equal to  $10 \text{ cm.s}^{-2}$  is missing in the recorded data. The gap is  
685 defined as the time elapsed between two consecutive observations including the missing  
686 records. Unlike the first method relying on inter-event times, this technique can detect gaps  
687 even when the stations recorded very few data. The list of the 189 stations that will be used in  
688 the testing is displayed in Table S2 (Supplementary Files). Figure 12 shows the gaps  
689 identified at two stations as examples. The method based on synthetic data identifies more  
690 gaps than the method based on inter-event times. The true lifetime is likely between these  
691 bounds. Corrected lifetimes of stations vary from a few month to 22 years at maximum.

692

693

### 694 **4.3 Testing results**

695

696 Mean hazard curves from the SHARE logic tree are considered. For a series of acceleration  
697 thresholds, the probability distributions for the number of sites with exceedance are obtained  
698 through Monte Carlo sampling, based on 10,000 runs (see the method in Section 2.2 and its  
699 application in France in Section 3.3). These distributions indicate the expected number of  
700 sites, out of the total number of sites, with at least one exceedance of the acceleration level  
701 over the total lifetime of the network.

702

703 At first, all 189 stations are considered (Fig. 10). The observed number of sites with  
704 exceedance is superimposed on the expected number of sites (Figs. 13a and 13b, red stars).  
705 Considering lifetimes corrected in Section 4.2.1 (1177 years in total), observations are  
706 consistent with the model, i.e. within the bounds of the distribution, for all acceleration  
707 thresholds greater than or equal to  $103 \text{ cm.s}^{-2}$  ( $>0.1g$ ). For highest levels,  $556$  and  $778 \text{ cm.s}^{-2}$ ,  
708 the test is not conclusive as there is no exceedance and the 2.5 percentile is also zero. At  $74$   
709  $\text{cm.s}^{-2}$ , the observed number of sites with exceedance (25) is slightly lower than the 2.5  
710 predicted percentile (26 sites). At the lowest level considered,  $53 \text{ cm.s}^{-2}$ , the observed number  
711 (29 sites) is much lower than the 2.5 predicted percentile (40 sites). Considering lifetimes  
712 corrected in Section 4.2.2 (892 years in total), comparable results are obtained, with observed  
713 values within the percentiles 2.5 and 97.5 for acceleration thresholds above  $53 \text{ cm.s}^{-2}$ . The  
714 observed numbers of sites with exceedance are identical, but the predicted numbers are  
715 decreased (as the total time window is decreased from 1177 to 892 years), resulting in a  
716 better fit between observed and predicted values. For information, the magnitudes and  
717 source-site distances of the earthquakes contributing to the threshold exceedances are  
718 reported in Fig. 14.

719

720 Imposing a minimum inter-site distances of 10 km, the number of stations is reduced from  
721 189 to 137. The results obtained for both sets of corrected lifetimes are very similar (compare  
722 Figs. 13a with 13c, Figs. 13b with 13d). The number of sites with exceedance (predicted and  
723 observed) decreases, but the fit between prediction and observations is identical. Imposing a  
724 minimum inter-site distance of 60 km (Figs. 13e and 13f), 49 sites are now considered. The  
725 total observation time window is strongly reduced, but the results are quite stable, with  
726 observations within the bounds of the predicted distribution for all acceleration levels  
727 considered (except at  $53 \text{ cm.s}^{-2}$  in Fig. 13e). Moreover, the list of earthquakes responsible for  
728 the threshold exceedances was systematically checked, to identify potential double counting.  
729 Discarding sites to ensure independence of sites brings minor changes to the plots and does  
730 not change the conclusions (Fig. 13, black stars).

731

## 732 5. CONCLUSIONS

733

734 We have carried out an extensive experiment to test probabilistic seismic hazard models  
735 against accelerometric datasets. A low-seismicity region, France, and a seismically active  
736 region, Turkey, are considered. Sites are sampled in space to compensate for the short  
737 observation time windows at accelerometric stations. Expected numbers of sites with  
738 exceedance, over the total observation time window, are compared to observed numbers of  
739 sites. A model is judged consistent with the observations if the observed number is within the  
740 percentiles 2.5 and 97.5 of the predicted distribution. The entire model is tested at once, the  
741 test provides an overall evaluation of the PSH model over a large geographical area.

742

743 As the maximum time window available is 16 years for the French RAP accelerometric  
744 database, the test is also carried out considering synthetic amplitudes based on an earthquake  
745 catalogue (LDG catalogue, 34 years) combined with a GMPE equation adapted to the French  
746 dataset (Cauzzi and Faccioli 2008). The tests led on true-recorded accelerations and on  
747 synthetic data provide comparable results. The AFPS2006 PSH model is consistent with the  
748 observations of the RAP network over the acceleration range 40-100  $\text{cm.s}^{-2}$  and for 50-200  
749 years return periods (62 sites, 449 yrs in total). When using synthetic accelerations over 34  
750 yrs at the same 62 sites (2108 yrs in total), the model predicts a number of sites with  
751 exceedance that is consistent with the “observations” over the range 40 to 130  $\text{cm.s}^{-2}$ . The  
752 MEDD2002 PSH model is provided all over France only for 4 return periods, from 100 to  
753 1975 years. For 100 years, there is only one site with exceedance, which is less than  
754 predicted. For longer return periods (475 and 975 years), the test led over the 16 years of the  
755 RAP network is not conclusive, since for these return periods both observed and predicted  
756 numbers equal zero. Using the synthetic dataset, the “observation” time window is increased.  
757 The model still over-predicts the observations at 100 years, but it is consistent with the  
758 observations for 475 and 975 years.

759

760 The results show that testing PSH models in France is at present very limited, as results are  
761 obtained only for low accelerations ( $\leq 0.1g$ ) which are not of real interest in earthquake  
762 engineering. Considering a series of acceleration thresholds, we show that results at a given  
763 acceleration level should not be extrapolated to higher levels. Testing PSH in France can be  
764 done only at low acceleration levels, and these results cannot be extrapolated to higher levels.  
765 Moreover, although AFPS2006 and MEDD2002 are providing different hazard curves  
766 (higher values in MEDD2002 than in AFPS2006), the observations available do not permit to

767 discriminate between these models. Both models are compatible with observations if  
768 considering the highest acceleration range or the highest return period range.

769

770 Applying the method in Turkey enable to test probabilistic seismic hazard estimates over an  
771 acceleration range useful for earthquake engineering. As the completeness issue is crucial,  
772 the recorded data at each station is analysed to detect potential gaps in the recording. Two  
773 techniques are proposed to identify gaps, and the tests are led considering both sets of  
774 corrected lifetimes. The maximum time window available is 22 years, stacking lifetimes at  
775 189 stations provides a time window of 1177 years (or 892 years). The PSH hazard estimates  
776 produced in the SHARE project (at rock) are considered. As most accelerometric stations are  
777 located on soil, the recorded PGA are converted to PGA at rock using the site-amplification  
778 published in Sandikkaya et al. (2013). The test is carried out considering all stations (189),  
779 then 137 stations with a minimum inter-site distance of 10km, and finally 49 stations with a  
780 minimum inter-site distance of 60km. These three sets of stations are considered, combined  
781 with the two sets of corrected lifetimes. The six tests provide comparable results, with  
782 observed numbers of sites with exceedance well within the bounds of the predicted  
783 distribution for accelerations between  $\sim 0.1$  and  $0.4g$ . For higher levels, both the observed  
784 number and the predicted percentile 2.5 are zero, and no conclusion can be drawn.

785

786 We are currently applying the same methodology to the French intensity database. Such  
787 study will enable to test ground motion levels of interest in earthquake engineering, recorded  
788 over longer time windows. However the results will also depend on some assumptions  
789 required, such as the completeness of intensity histories at sites, or the conversion of intensity  
790 into acceleration. In the future, another type of observation could be used to constrain the  
791 hazard curves, precarious rocks or other fragile geological features such as speleothems  
792 (Anderson et al. 2011). Maximum acceleration levels over given time windows could thus be  
793 constrained. Any testing method relies on some assumptions, and the discrepancies between  
794 observations and predictions can generally have more than one explanation. We believe that  
795 firm conclusions on the validity of a PSH model will only be possible if applying for the  
796 same region several techniques, using different observables, recorded over different time  
797 windows.

798

799

800



## 801 **Data and Resources**

802

803 The accelerometric database built within this article is based on data available online (French  
804 Accelerometric Network, <http://www-rap.obs.ujf-grenoble.fr/>, last accessed May 2013). The  
805 Rennass earthquake catalogue is provided by the Réseau National de Surveillance Sismique  
806 (RéNaSS, <http://renass.u-strasbg.fr/>, last accessed May 2013). The LDG earthquake  
807 catalogue (2012) is provided by LDG upon request.

808

809 The SHARE seismic hazard map is available at [www.efehr.org](http://www.efehr.org). The Turkish accelerometric  
810 data is available at <http://kyh.deprem.gov.tr/ftpe.htm>. The following catalogues have been  
811 used in the present paper: International Seismological Centre online bulletin,  
812 <http://www.isc.ac.uk/iscbulletin/search/bulletin/> (last accessed April 2014), and GCMT  
813 earthquake catalogue, <http://www.globalcmt.org/CMTsearch.html> (last accessed April 2014).  
814 The SHEEC earthquake catalogue can be find at <http://www.emidius.eu/SHEEC/> (last  
815 accessed May 2014), and the catalog of B.Ü. KOERI National Earthquake Monitoring Center  
816 can be find at [www.koeri.boun.edu.tr](http://www.koeri.boun.edu.tr) (last accessed May 2014).

817

818

819

## 820 **Acknowledgments**

821

822 The authors thank the Editor Egill Hauksson, Mark Stirling and an anonymous reviewer for  
823 their helpful and constructive reviews of the manuscript. Hilal Tasan's PhD grant is funded  
824 by the Seismic Ground Motion Assessment project (SIGMA, [projet-sigma.com](http://projet-sigma.com)). We are  
825 grateful to the Laboratoire de Détection et de Géophysique (LDG) for sharing the earthquake  
826 catalogue. We are thankful to Pierre-Yves Bard for fruitful discussions. Aida Azari Sisi  
827 (METU) kindly contributed in the processing of the accelerometric data. ISTerre laboratory is  
828 part of LabEx OSUG@2020 (ANR10 LABX56).

829

## 830 **References**

831

- 832 Akkar, S. & Bommer, J.J., 2010. Empirical Equations for the Prediction of PGA, PGV, and Spectral  
833 Accelerations in Europe, the Mediterranean Region, and the Middle East., *Seism. Res. Lett.*, 81,  
834 195–206.
- 835 Akkar, S. & Çağnan, Z., 2010. A Local Ground-Motion Predictive Model for Turkey, and Its  
836 Comparison with Other Regional and Global Ground-Motion Models. *Bull. seism. Soc. Am*, 100  
837 (6 ), 2978–2995. doi:10.1785/0120090367
- 838 Akkar, S., Çağnan, Z., Yenier, E., Erdoğan, Ö., Sandikkaya, M. A., & Gülkan, P., 2010. The recently  
839 compiled Turkish strong motion database: preliminary investigation for seismological  
840 parameters. *J. Seism.*, 14(3), 457–479.
- 841 Akkar, S., Sandikkaya, M. A., Şenyurt, M., Azari Sisi, A., Ay, B. Ö., Traversa, P., Douglas, J., et al. ,  
842 2014. Reference database for seismic ground-motion in Europe (RESORCE). *Bull. seism. Soc.*  
843 *Am*, 12(1), 311–339.
- 844 Albarello, D. & D’Amico, V., 2008. Testing probabilistic seismic hazard estimates by comparison  
845 with observations: an example in Italy., *Geophys. J. Int.*, 175, 1088–1094.
- 846 Anderson, J. G., Brune, J. N., Biasi, G., Anooshehpour, A. & Purvance, M., 2011. Workshop Report:  
847 Applications of Precarious Rocks and Related Fragile Geological Features to US National  
848 Hazard Maps. *Seism. Res. Lett*, 82(3), 431-441.
- 849 Atkinson, G. M. & Boore, D. M., 2011. Modifications to existing ground-motion prediction equations  
850 in light of new data. *Bull. seism. Soc. Am.*, 101(3), 1121-1135.
- 851 Beauval, C. & Scotti, O., 2004. Quantifying Sensitivities of PSHA for France to Earthquake Catalog  
852 Uncertainties, Truncation of Ground-Motion Variability, and Magnitude Limits., *Bull. seism.*  
853 *Soc. Am.*, 94, 1579–1594.
- 854 Beauval, C., Bard, P.-Y., Hainzl, S. & Guéguen, P., 2008. Can Strong-Motion Observations be Used  
855 to Constrain Probabilistic Seismic-Hazard Estimates?, *Bull. seism. Soc. Am.*, 98, 509–520.
- 856 Beauval, C., Tasan, H., Laurendeau, A., Delavaud, E., Cotton, F., Guéguen, P. & Kuehn, N., 2012.  
857 On the Testing of Ground-Motion Prediction Equations against Small-Magnitude Data., *Bull.*  
858 *seism. Soc. Am.*, 102, 1994–2007.
- 859 Boore, D.M. & Atkinson, G.M., 2008. Ground-Motion Prediction Equations for the Average  
860 Horizontal Component of PGA, PGV, and 5%-Damped PSA at Spectral Periods between 0.01s  
861 and 10.0s., *Earthq. Spectra*, 24, 99.
- 862 Bozkurt, E., 2001. Neotectonics of Turkey—a synthesis. *Geodin. Acta*, 14(1), 3-30.
- 863 Campbell, K.W., 1997. Empirical near-source attenuation relationships for horizontal and vertical  
864 components of peak ground acceleration, peak ground velocity, and pseudo-absolute  
865 acceleration response spectra. *Seismol. Res. Lett.*, 68:154–179.
- 866 Chiou, B. S.-J. & Youngs, R. R., 2008. An NGA Model for the Average Horizontal Component of  
867 Peak Ground Motion and Response Spectra. *Earthq. Spectra*, 24, 173-215.

- 868 Cornell, C.A., 1968. Engineering seismic risk analysis., *Bull. seism. Soc. Am.*, 58, 1583–1606.
- 869 Cauzzi, C. & Faccioli, E., 2008. Broadband (0.05 to 20 s) prediction of displacement response spectra  
870 based on worldwide digital records., *J. Seism.*, 12, 453–475.
- 871 Delavaud, E., Cotton, F., Akkar, S., Scherbaum, F., Danciu, L., Beauval, C., Drouet, S., Douglas, J.,  
872 Basili, R., Sandikkaya, M.A., Segou, M., Faccioli, E. & Theodoulidis, N., 2012, Toward a  
873 Ground-Motion Logic Tree for Probabilistic Seismic Hazard Assessment in Europe, *J. Seis.*,  
874 doi:10.1007/s10950-012-9281-z.
- 875 Drouet, S., Cotton, F. & Guéguen, P., 2010. vS30,  $\kappa$ , regional attenuation and Mw from  
876 accelerograms: application to magnitude 3-5 French earthquakes., *Geophys. J. Int.*, 182, 880–  
877 898.
- 878 Frohlich, C. & Apperson, K. D., 1992. Earthquake focal mechanisms, moment tensors, and the  
879 consistency of seismic activity near plate boundaries, *Tectonics*, 11(2), 279–296.
- 880 Fujiwara, H., Morikawa, N., Ishikawa, Y., Okumura, T., Miyakoshi, J., Nojima, N. & Fukushima, Y.,  
881 2009. Statistical Comparison of National Probabilistic Seismic Hazard Maps and Frequency of  
882 Recorded JMA Seismic Intensities from the K-NET Strong-motion Observation Network in  
883 Japan during 1997–2006., *Seism. Res. Lett.*, 80, 458–464.
- 884 Giardini, D., Woessner, J., Danciu, L., Crowley, H., Cotton, F., Grünthal, G., Pinho, R., Valensise, G.,  
885 Akkar, S., Arvidsson, R., Basili, R., Cameelbeeck, T., Campos-Costa, A., Douglas, J.,  
886 Demircioglu, M.B., Erdik, M., Fonseca, J., Glavatovic, B., Lindholm, C., Makropoulos, K.,  
887 Meletti, C., Musson, R., Pitilakis, K., Sesetyan, K., Stromeyer, D., Stucchi, M. & Rovida, A.,  
888 Seismic Hazard Harmonization in Europe (SHARE): Online Data Resource,  
889 doi: 10.12686/SED-00000001-SHARE, 2013.
- 890 Grünthal, G., Wahlström, R. & Stromeyer, D., 2013. The SHARE European Earthquake Catalogue  
891 (SHEEC) for the time period 1900–2006 and its comparison to the European-Mediterranean  
892 Earthquake Catalogue (EMEC). *J. Seism.*, 17(4), 1339–1344. doi:10.1007/s10950-013-9379-y.
- 893 Iervolino I., 2013. Probabilities and Fallacies: Why Hazard Maps Cannot Be Validated by Individual  
894 Earthquakes, *Earthq. Spectra*, Volume 29, No. 3, pages 1125–1136.
- 895 Laboratoire de Détection et de Géophysique (LDG), 2012. Catalog of French seismicity 1962-2011,  
896 CEA/Laboratoire de Détection et de Géophysique, Bruyères-le-Châtel, France.
- 897 Leonard, M., 2010. Earthquake Fault Scaling: Self-Consistent Relating of Rupture Length, Width,  
898 Average Displacement, and Moment Release. *Bull. seism. Soc. Am.*, 100 (5A ), 1971–1988.
- 899 Martin, Ch., Combes, P., Secanell, R., Lignon, G., Carbon, D., Fioravanti, A. and Grellet, B., 2002.  
900 Révision du zonage sismique de la France: étude probabiliste, under the supervision of the  
901 Groupe d'Etude et de Proposition pour la Prévention du risque sismique en France and the  
902 Association Française du Génie Parasismique (in French)., Geoter Report, GTR/MATE/0701-  
903 150.

- 904 Martin, Ch. & Secanell, R., 2006. Développement d'un modèle probabiliste d'aléa sismique calé sur  
905 le retour d'expérience, Phase 2: Calculs et cartographie suivant l'arbre logique défini par le  
906 groupe « zonage », Document GZ7 produit dans le cadre du groupe de travail AFPS « ZONAGE  
907 », Geoter Report, GTR/CEA/0306-294, 39 pages (in French).
- 908 McGuire, R.K., 1976. FORTRAN computer program for seismic risk analysis, U.S. Geological  
909 Survey Open-File Report 76-67.
- 910 Mucciarelli, M., Albarello, D. & D'Amico, V., 2008. Comparison of Probabilistic Seismic Hazard  
911 Estimates in Italy., *Bull. seism. Soc. Am.*, 98, 2652–2664.
- 912 Musson, R.M.W. & Winter, P.W., 2011. Objective assessment of source models for seismic hazard  
913 studies: with a worked example from UK data, *Bull. Earthq. Eng.*, DOI 10.1007/s10518-011-  
914 9299-6.
- 915 Papazachos, B.C., 1990. Seismicity of the Aegean and surrounding area., *Tectonophysics*, 178, 287–  
916 308.
- 917 Pequegnat, C., Gueguen, P., Hatzfeld, D. & Langlais, M., 2008. The French Accelerometric Network  
918 (RAP) and National Data Centre (RAP-NDC)., *Seism. Res. Lett.*, 79, 79–89.
- 919 Reasenber, P., 1985. Second-order moment of central California seismicity, 1969–1982., *J. Geophys.*  
920 *Res.Solid Earth*, 90, 5479–5495.
- 921 Régnier, J., Laurendeau, A., Duval, A.-M., & Gueguen, P., 2010. From heterogeneous set of soil data  
922 to Vs profile: Application on the French permanent accelerometric network (RAP) sites, in  
923 Proceedings Fourteenth ECEE—European Conference of Earthquake Engineering, Ohrid,  
924 Republic of Macedonia, Paper ID 851.
- 925 Rhoades, D., Smith, W.D. & Stirling, M.W., 2002. Tests of seismic hazard models, GNS Consultancy  
926 Report for Earthquake Commission Research Foundation, Project No. 01/460, 43 pages.
- 927 Sandikkaya, M. A., Akkar, S. & Bard, P., 2013. A Nonlinear Site-Amplification Model for the Next  
928 Pan-European Ground-Motion Prediction Equations, *Bull. seism. Soc. Am.*, 103 (1), 19–32.  
929 doi:10.1785/0120120008.
- 930 Sandikkaya, M. A., Yılmaz, M., Bakır, B. S., & Yılmaz, Ö., 2010. Site classification of Turkish  
931 national strong-motion stations. *J. Seism*, 14(3), 543–563. doi:10.1007/s10950-009-9182-y.
- 932 Scherbaum, F., Cotton, F. & Smit, P., 2004. On the Use of Response Spectral-Reference Data for the  
933 Selection and Ranking of Ground-Motion Models for Seismic-Hazard Analysis in Regions of  
934 Moderate Seismicity: The Case of Rock Motion., *Bull. seism. Soc. Am.*, 94, 2164–2185.
- 935 Sesetyan K., Demircioglu, M., Rovida, A., Albini, P. & Stucchi, M., 2013. SHARE-CET, the SHARE  
936 earthquake catalogue for Central and Eastern Turkey complementing the SHARE European  
937 Earthquake Catalogue (SHEEC), 4 pages,  
938 [http://www.emidius.eu/SHEEC/docs/SHARE\\_CET.pdf](http://www.emidius.eu/SHEEC/docs/SHARE_CET.pdf), last accessed 2014, May 7<sup>th</sup>.

- 939 Sollogoub, P., Bard, P.-Y., Hernandez, B., Jalil, W., Labbé, P., Mouroux, P. & Viallet, E., 2007.  
940 Rapport du groupe de travail “Zonage”, Association Française de génie Parasismique (AFPS),  
941 58 pp. (in French, available on request).
- 942 Stein, S., Geller, R. & Liu, M., 2011. Bad Assumptions or Bad Luck: Why Earthquake Hazard Maps  
943 Need Objective Testing?, *Seism. Res. Lett.*, 82, 623–626.
- 944 Stirling, M.W., 2012. Earthquake Hazard Maps and Objective Testing: The Hazard Mapper’s Point of  
945 View., *Seism. Res. Lett.*, 83, 231–232.
- 946 Stirling, M. & Gerstenberger, M., 2010. Ground Motion–Based Testing of Seismic Hazard Models in  
947 New Zealand., *Bull. seism. Soc. Am.*, 100, 1407–1414.
- 948 Stirling, M. & Petersen, M., 2006. Comparison of the Historical Record of Earthquake Hazard with  
949 Seismic- Hazard Models for New Zealand and the Continental United States., *Bull. seism. Soc.*  
950 *Am.*, 96, 1978–1994.
- 951 Strasser, F.O., Abrahamson, N.A. & Bommer, J.J., 2009. Sigma: Issues, Insights, and Challenges.,  
952 *Seism. Res. Lett.*, 80, 40–56.
- 953 Ward, S.N., 1995. Area-based tests of long-term seismic hazard predictions. *Bull. seism. Soc., Am.*,  
954 85, 1285–1298.
- 955 Yenier, E., M.A. Sandikkaya, & Akkar, S., (2010). Report on the fundamental features of the  
956 extended strong-motion databank prepared for the SHARE Project, Workshop for WP4, Ankara,  
957 Turkey ([www.share-eu.org/sites/default/files/D4%201\\_SHARE.pdf](http://www.share-eu.org/sites/default/files/D4%201_SHARE.pdf) last accessed on April 2014).
- 958 Yılmaz, Ö., Savaşkan, E., Bakır, B. S., Yılmaz, M. T., Eser, M. , Akkar, S., Tüzel, B., İravul, Y.,  
959 Özmen, Ö. T., Denizlioğlu, A. Z., Alkan, A., & Gürbüz, M. 2008. Shallow Seismic and  
960 Geotechnical Site Surveys at the Turkish National Grid for Strong-Motion Seismograph  
961 Stations., *14th World Conference on Earthquake Engineering*, Beijing.
- 962 Zhao, J. X., Zhang, J., Asano, A., Ohno, Y., Oouchi, T., Takahashi, T., Ogawa, H., Irikura, K., Thio,  
963 H. K., Somerville, P. G., Fukushima, Y. & Fukushima, Y., 2006. Attenuation relations of strong  
964 ground motion in Japan using site classification based on predominant period. *Bull. seism. Soc.*,  
965 *Am*, 96 (3), 898–913.

966  
967  
968  
969

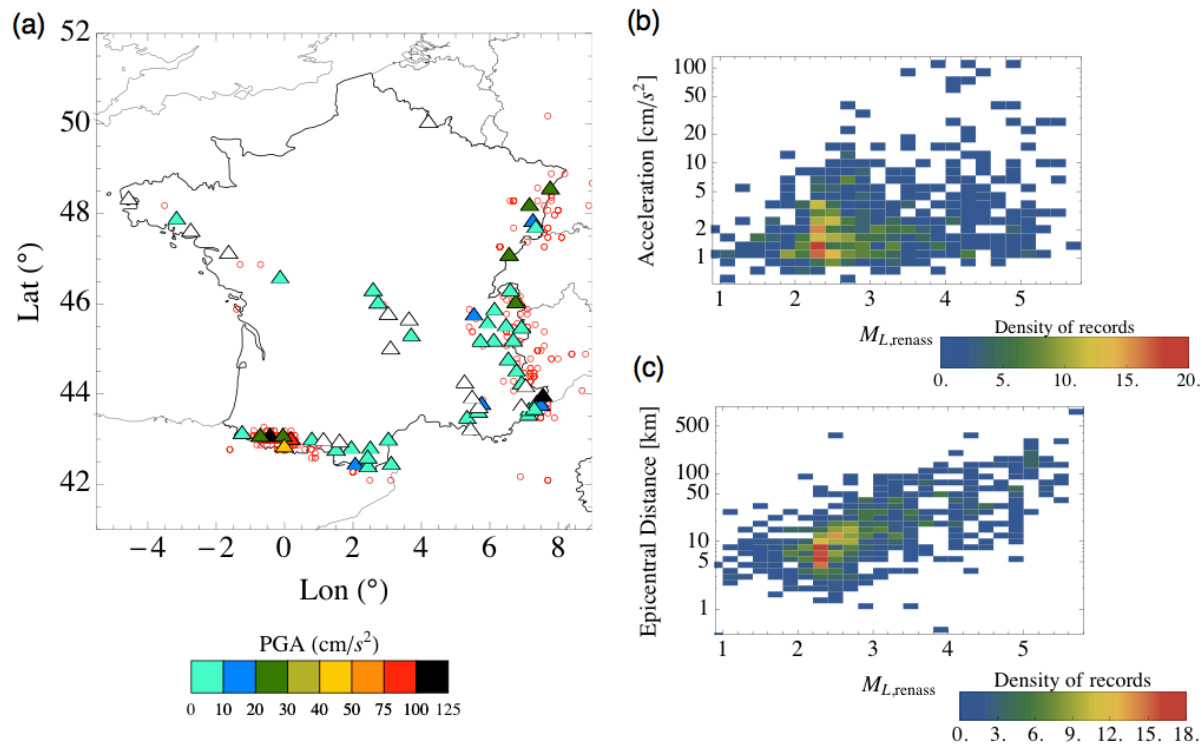
970 **Figures**  
971

Site	$t_{obs}$ yr	$\lambda_{25cm/s^2}$ , rate	$N_{mean}$	Probability distribution for the number of exceedances of 25 cm/s <sup>2</sup>	Sampling the distribution: numbers of exceedances					
					Run n°1	Run n°2	Run n° 3	...	Run n° 10 <sup>4</sup>	
<b>OGTI</b>	13.52	0.0429	0.580	Mean= 0.580 	=>	1	0	1	...	0
<b>PYAD</b>	7.91	0.1748	1.380	Mean= 1.380 	=>	2	4	1	...	1
<b>STBO</b>	9.86	0.0309	0.305	Mean= 0.305 	=>	0	1	0	...	0
<b>SAOF</b>	16.26	0.0557	0.906	Mean= 0.906 	=>	1	1	0	...	2
<b>QUIF</b>	6.16	0.0122	0.075	Mean= 0.075 	=>	0	1	0	...	1
<b><math>\Sigma t_{OBS} = 53.7</math> yrs</b>						↓	↓	↓	...	↓
a)				<=	$N_{EXC}$ number of exceedances	4	7	2	...	4
b)				<=	$N_{SITES}$ Number of sites with exceedances	3	4	2	...	3

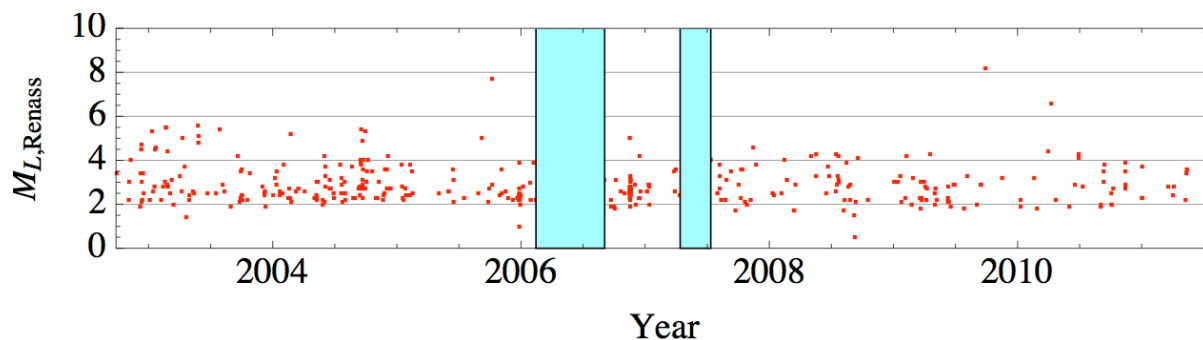
972  
973 **Figure 1:** Scheme detailing the Monte Carlo process followed for generating a) the probability  
974 distribution for the number of exceedances ( $N_{EXC}$ ) considering all sites, b) the probability  
975 distribution for the number of sites with at least one exceedance ( $N_{SITES}$ ). The acceleration threshold is fixed (25  
976 cm/s<sup>2</sup>). Five accelerometric sites are considered in this example, with different lifetimes, resulting in a  
977 total observation time window of 55 years. The probability distributions provide numbers of  
978 occurrences over 55 years.  $t_{OBS}$ : observation time length of the stations,  $\lambda_{25cm/s^2}$ : predicted annual rate of

979 exceeding  $25\text{cm/s}^2$ ,  $N_{\text{mean}}$ : Predicted number of exceedances for a ground motion higher than or equal  
 980 to  $25\text{cm/s}^2$  during  $t_{\text{OBS}}$ .

981  
 982  
 983  
 984

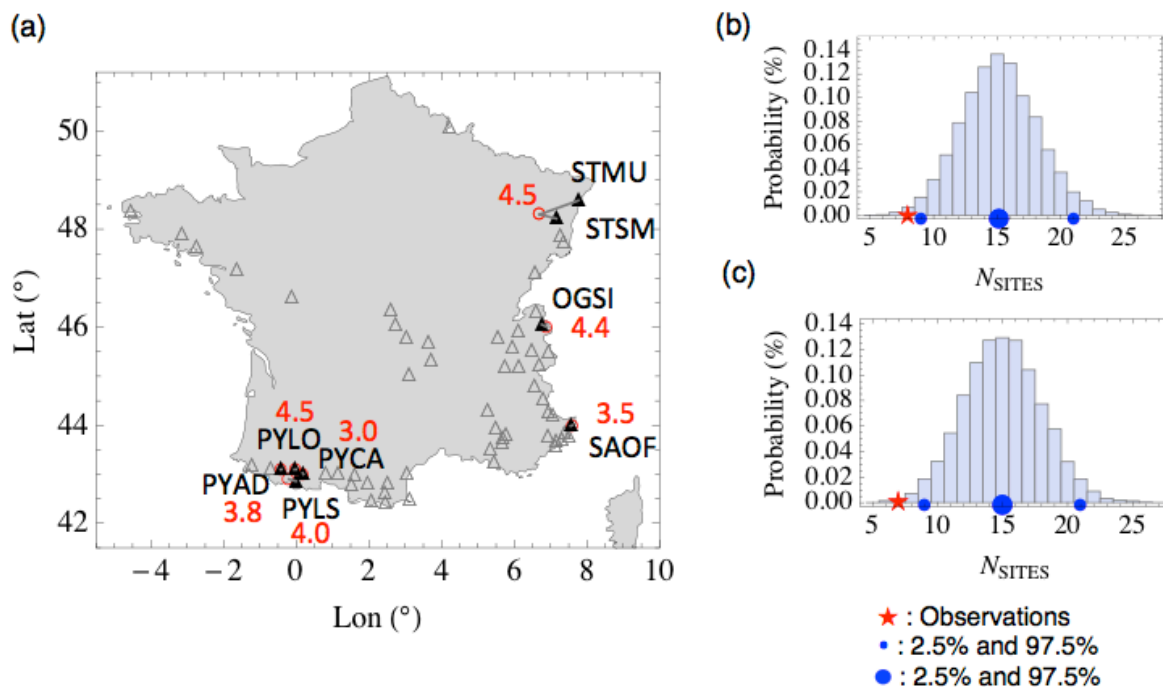


985 **Figure 2:** The accelerometric dataset built from the RAP raw database, for testing PSHA in France. (a)  
 986 Coloured triangles: the 47 rock stations which have experienced at least one  $\text{PGA} \geq 1 \text{ cm/s}^2$  during their lifetime,  
 987 white triangles: 15 remaining rock stations. Colour scale: maximum acceleration recorded at each station.  
 988 Circles: responsible earthquakes. (b) Distribution of all PGA amplitudes against the magnitude of the  
 989 corresponding earthquake ( $M_{L,\text{Renass}}$ ). (c) Distribution of epicentral distances of the records against the  
 990 magnitude of the corresponding earthquake.  
 991  
 992  
 993  
 994



995 **Figure 3:** Detecting gaps in the observation lifetimes of RAP stations, example at station PYOR.  
 996 Magnitude of the earthquake associated to the accelerometric record versus time. Original observation  
 997 lifetime: 8.8 years. Shading : two gaps identified (inter-event times  $> 10 * \text{average inter-event time}$ ).  
 998 Corrected lifetime : 8.0 years.  
 999

1000  
 1001  
 1002  
 1003

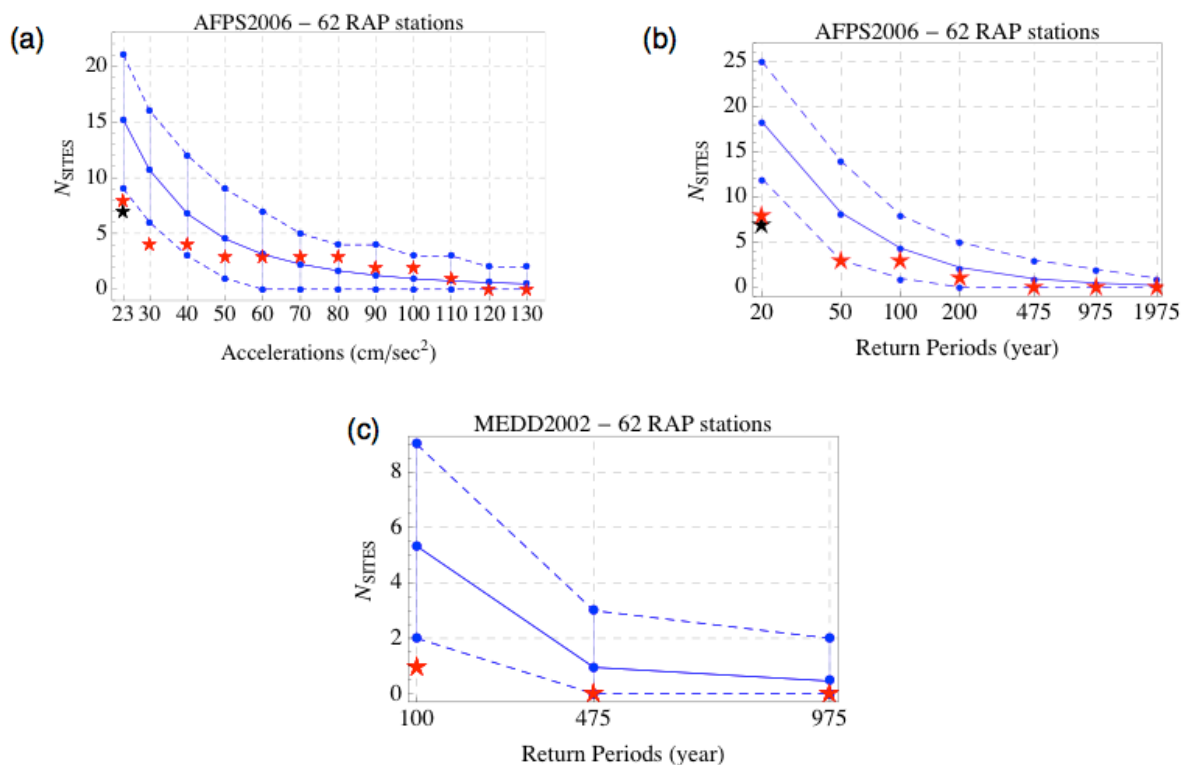


1004

1005 **Figure 4:** Testing the AFPS2006 model against the accelerometric dataset, example for the  
 1006 acceleration threshold  $A_0 = 23 \text{ cm/s}^2$ . (a) Locations of the 8 stations, out of 62, which recorded a  
 1007 ground motion higher than  $A_0$  (black filled triangles, acronyms of stations indicated), and responsible  
 1008 events (circles,  $M_w$  indicated). Right: b) the observed number of sites where  $A_0$  was exceeded is  
 1009 superimposed on the probability distribution predicted by the PSH model. In this example, the model  
 1010 over-predicts the observations; c) two records producing exceedance are related to the same  
 1011 earthquake (stations STMU and STSM), excluding one station from the analysis does not change the  
 1012 conclusions (predictions are for 61 stations).

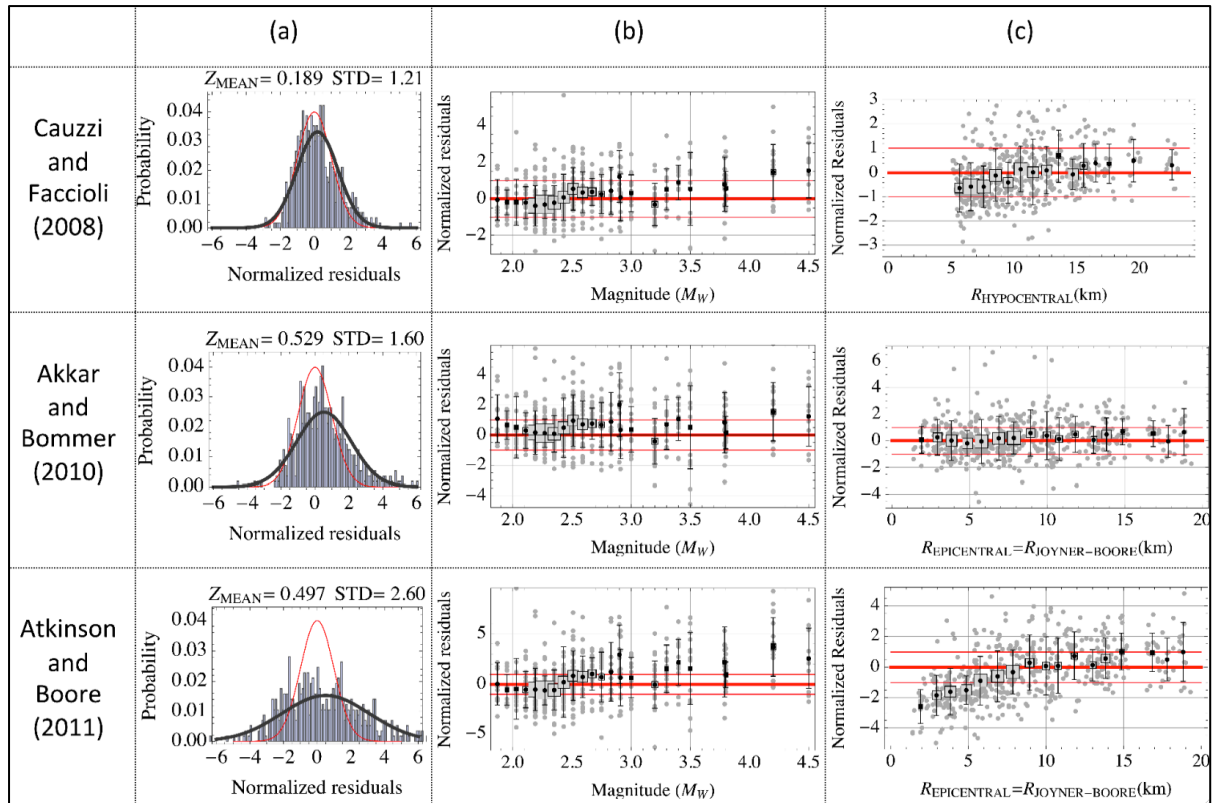
1013  
 1014  
 1015  
 1016





1017  
1018  
1019

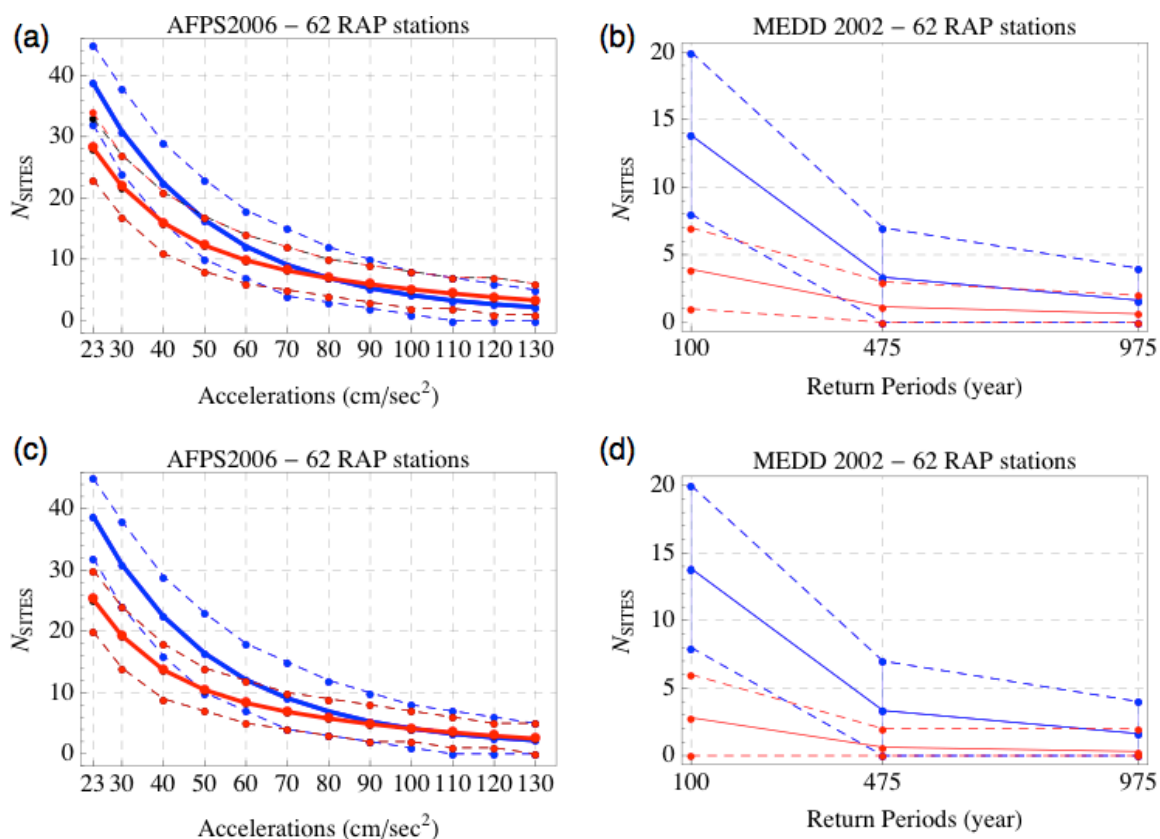
1020 **Figure 5:** Testing the probabilistic seismic hazard models against accelerometric data in France:  
1021 predicted and observed number of sites with exceedance (62 rock sites, total time window 449 years).  
1022 Blue curves: median and percentiles 2.5 and 97.5 of the predicted distributions, red stars: observed  
1023 number of sites. Black stars: reduced number of sites in the case of double counting (see Fig. 4). (a)  
1024 Results for the AFPS2006 PSH model, considering a range of acceleration thresholds. (b) Results for  
1025 the AFPS2006 PSH model, considering a range of return period thresholds. (c) Results for  
1026 MEDD2002 model, considering 3 return periods.



1027

1028 **Figure 6:** Testing 3 ground-motion prediction models against the newly built accelerometric French  
 1029 dataset. Column A: histogram of residuals superimposed on the standard normal distribution  
 1030 representing the model (red curve), a residual corresponds to  $[\text{Log}(\text{observation}) -$   
 1031  $\text{Log}(\text{prediction})]/\sigma$ . Column B: distribution of residuals versus magnitude (0.1 magnitude  
 1032 binning). Column C: distribution of the residuals with respect to source-site distance (1km distance  
 1033 binning). Squares: mean of residuals, size proportional to the number of residuals falling in each bin,  
 1034 error bars correspond to  $\pm 1$  standard deviation of model (normalized residuals). ( $Z_{MEAN}$ : Mean  
 1035 normalized residuals, STD: Standard deviation of normalized residuals.)  
 1036

1037



1038

1039

1040

1041

1042 **Figure 7:** Application in France, testing the PSH models against synthetic accelerometric data:  
 1043 predicted and “observed” number of sites with at least one exceedance (62 rock sites with 34 years,  
 1044 total time window 2108 years). Blue curves: predicted distributions, mean and percentiles 2.5 and  
 1045 97.5. Red curves: observed distributions, mean and percentiles 2.5 and 97.5. Black curves: reduced  
 1046 number of sites in the case of double counting. The synthetic data were generated using the LDG  
 1047 catalogue and sampling the Gaussian of the CF2008 GMPE between  $\pm 3\sigma$ . (a) AFPS2006 model. (b)  
 1048 MEDD2002 model, considering 3 return periods. (c) and (d): same as (a) and (b) but sampling the  
 1049 CF2008 GMPE between  $\pm 2\sigma$  (see the text).

1050

1051

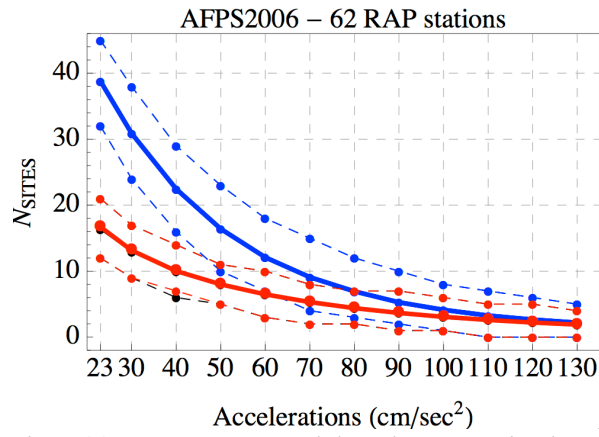
1052

1053

1054

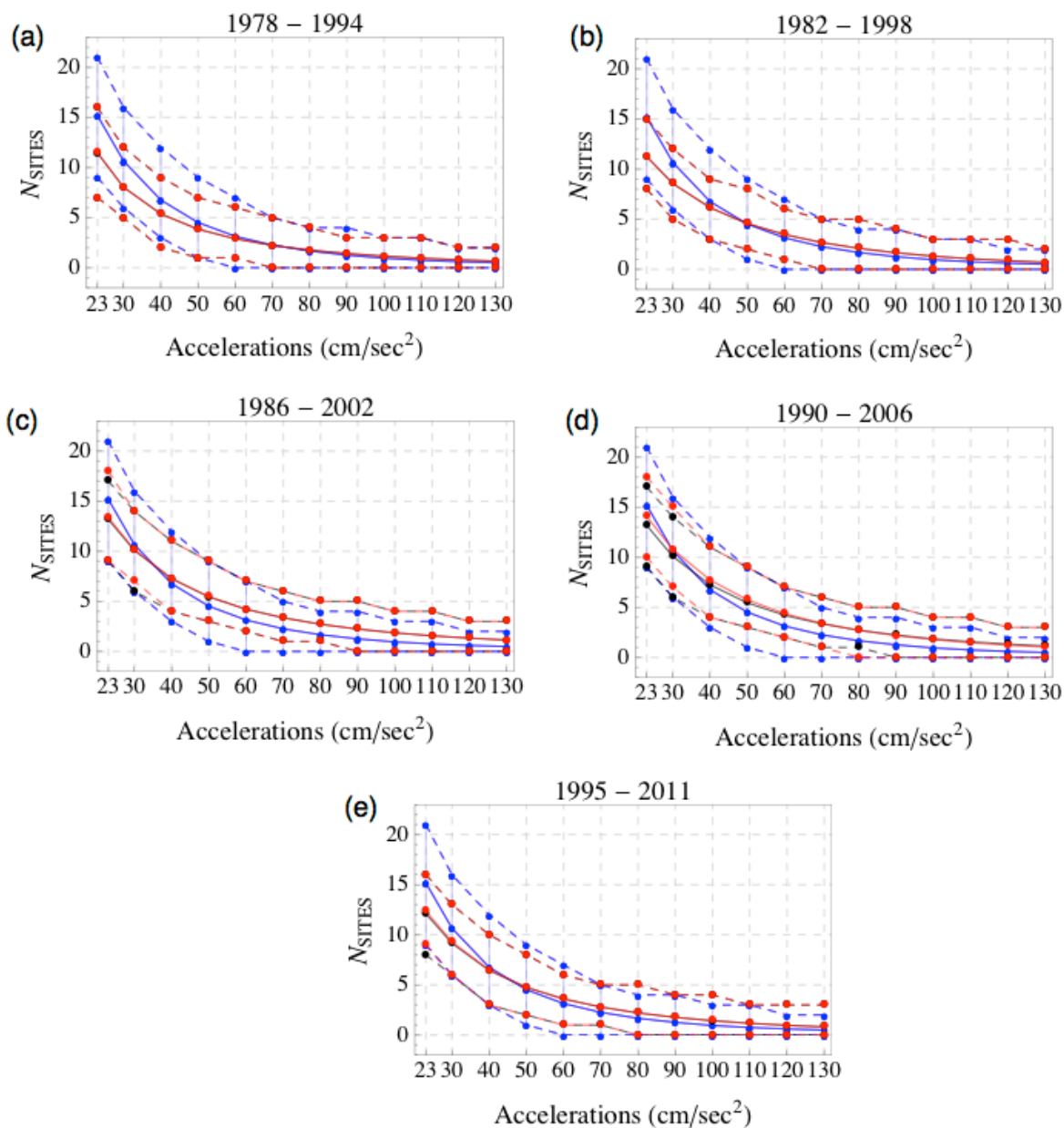
1055

1056



1057  
1058  
1059  
1060  
1061  
1062  
1063  
1064

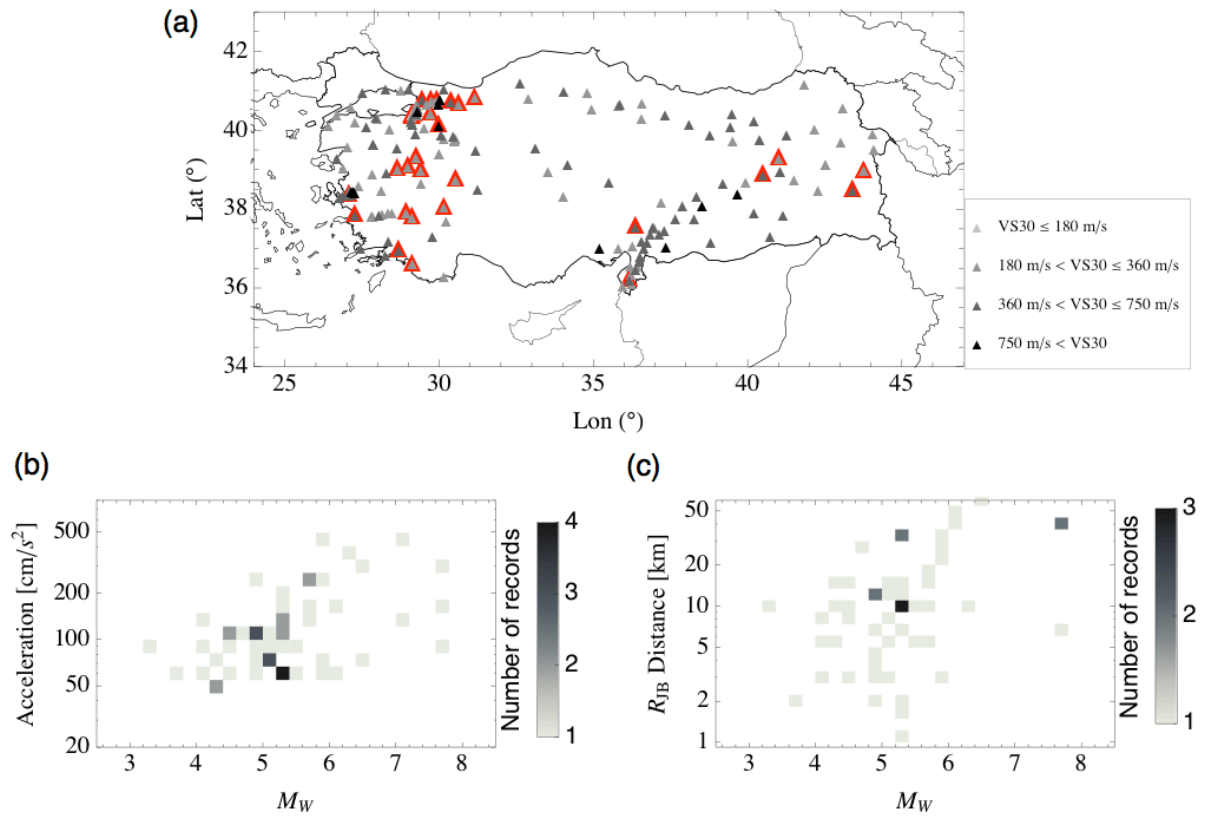
**Figure 8:** See legend of Fig. 7(a). AFPS2006 model, only events in the LDG earthquake catalogue with  $M_{L,LDG} \geq 3.5$  are used for generating synthetic data, sampling the Gaussian of the CF2008 GMPE between  $\pm 3\sigma$ .



1065  
 1066  
 1067  
 1068  
 1069  
 1070  
 1071  
 1072  
 1073  
 1074  
 1075  
 1076  
 1077  
 1078

**Figure 9:** Testing AFPS2006 model against synthetic accelerometric data at 62 sites in France, and evaluating the stability of the results, with respect to the time window used. Five sliding windows are considered between 1978 and 2011, with length equal to the lifetime of the RAP network (16 yrs). Each station is attributed the same lifetime as in the real case. For each 16-yr period, synthetic datasets are generated by coupling the LDG catalogue with the GMPE CF2008 (sampled between  $\pm 3\sigma$ ). Total observation time window is 449 years, like in the real case.

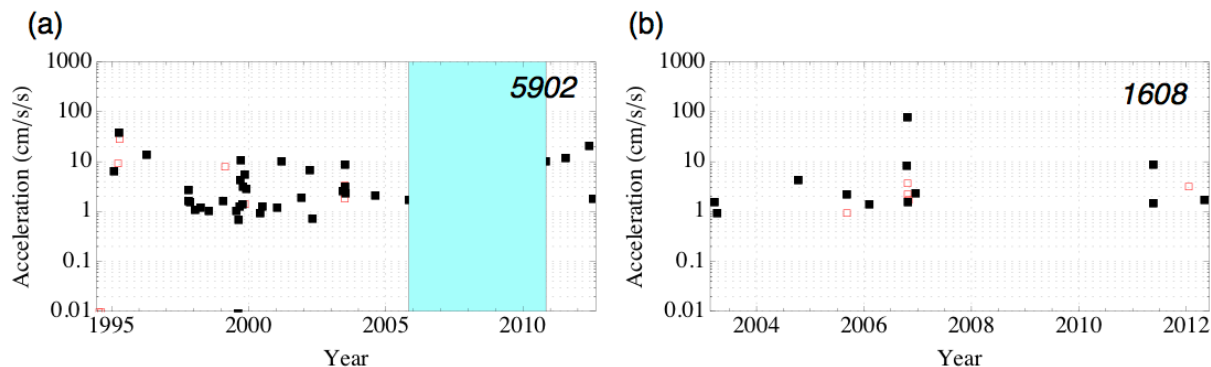
1079



1080

1081 **Figure 10:** Location of Turkish stations and content of the final database used for testing. (a) 189  
 1082 accelerometric stations, with known  $V_{S30}$  values. Triangles: stations used in the testing ( $V_{S30}$   
 1083 indicated). Red Triangles: 30 stations (out of 189) that observed a median  $PGA_{ROCK} \geq 50 \text{ cm.s}^{-2}$ . (b)  
 1084 Distribution of the 56 records with  $PGA_{ROCK} \geq 50 \text{ cm.s}^{-2}$  recorded at 30 stations, in terms of PGA  
 1085 versus  $M_w$  of the earthquake ; (c) in terms of epicentral distance versus  $M_w$ .

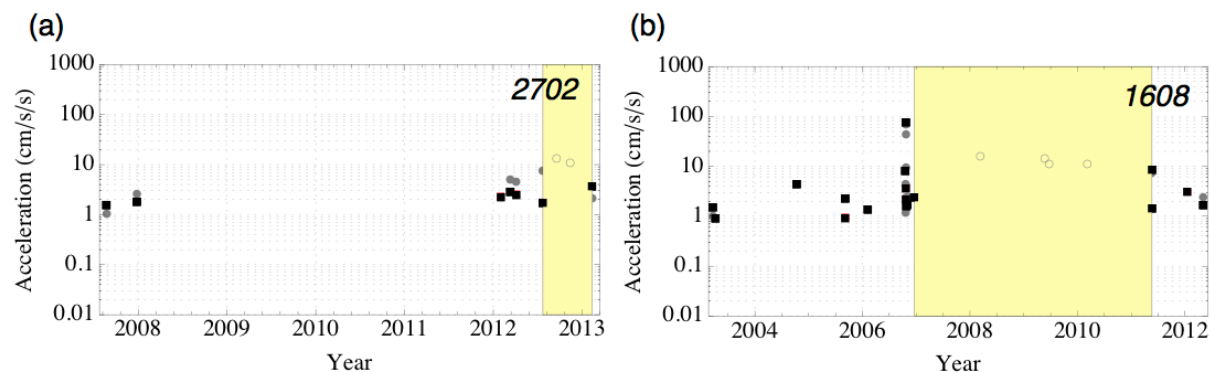
1086



1087  
1088

1089 **Figure 11:** Identification of gaps at Turkish stations using average inter-event times (raw data,  
1090 Section 4.2.1), example at two stations. (a) Time history at station 5902 (lifetime 18.03 years); shaded  
1091 area : gap identified (5 years). (b) Time history at station 1608, no gap identified. Solid squares :  
1092 observed PGA from mainshocks, red square : observed PGA from foreshocks/aftershocks.

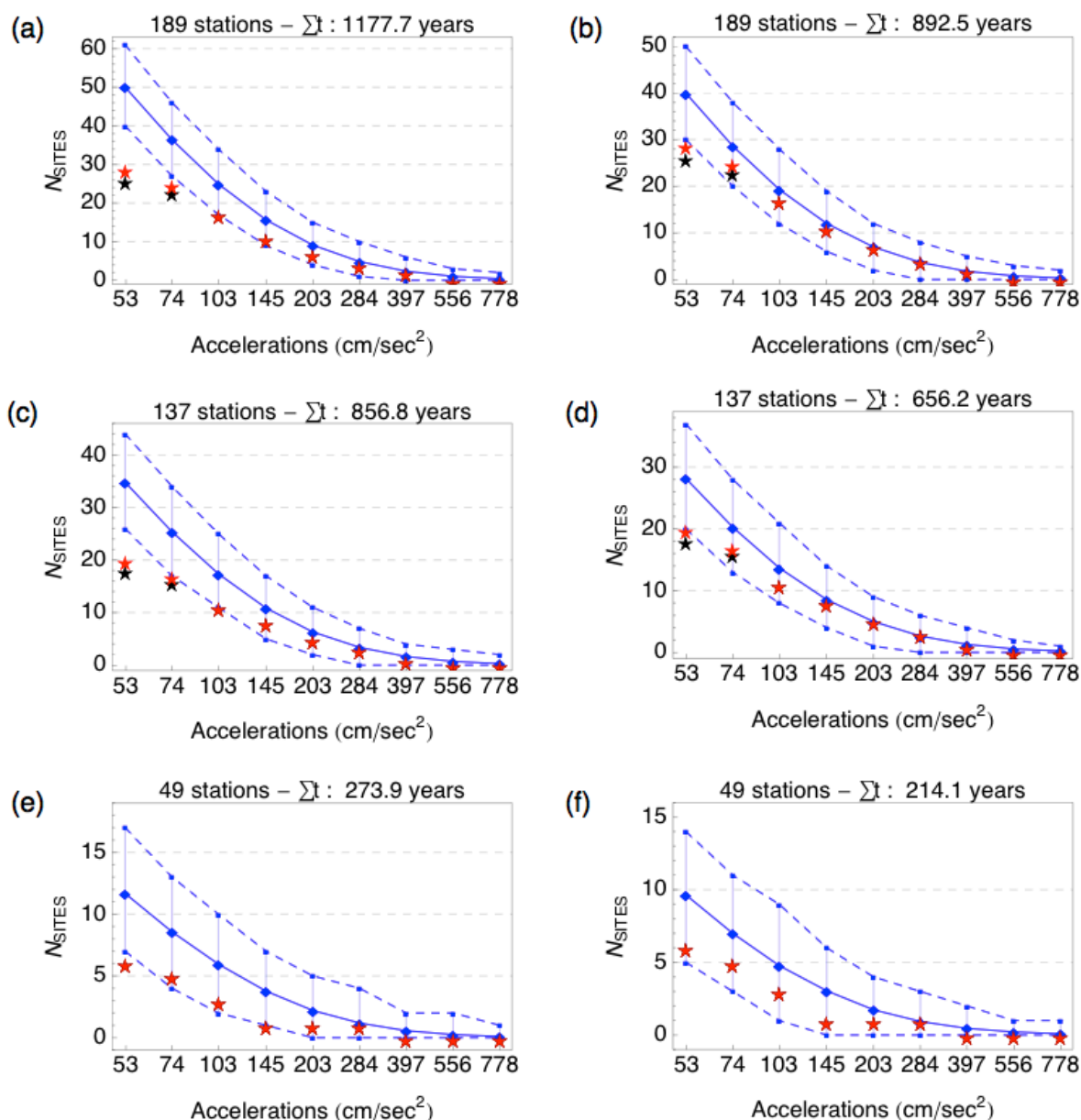
1093  
1094



1095  
1096

1097 **Figure 12:** Identifying gaps in operating lifetime of stations (second method, Section 4.2.2), example  
1098 at 2 Turkish stations (n° 2702 and n° 1608.). Black squares: observed PGA, grey circles: predicted  
1099 PGA for events in the database, plain circles: predicted PGA  $\geq 10$  cm.s<sup>-2</sup> missing in the database.  
1100 Shaded time window: identified gap. Synthetic PGA are generated at each site by combining the  
1101 Turkish earthquake catalogue and a GMPE (Akkar and Cagnan 2010).

1102  
1103



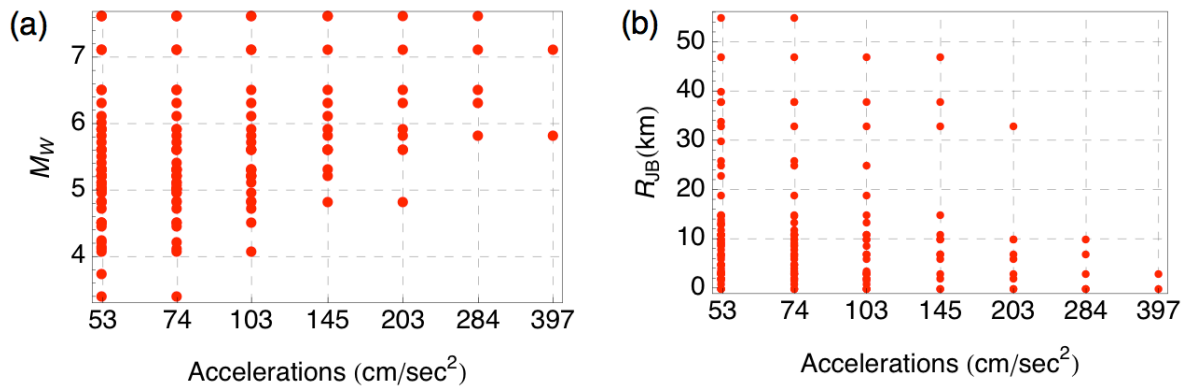
1104

1105

1106 **Figure 13:** Testing PSHA in Turkey, comparison of the observed and predicted number of sites with  
 1107 exceedance at different acceleration levels, over the observation lifetime of the network. Predicted  
 1108 numbers are based on the SHARE hazard curves. (a) 189 stations, 1<sup>st</sup> set of corrected lifetimes (1177  
 1109 years in total); (b) 189 stations, 2<sup>nd</sup> set of corrected lifetimes (889 years in total). (c) and (d): same as  
 1110 (a) and (b) with 137 stations with minimum inter-site distance of 10 km (856 and 656 years in total).  
 1111 (e) and (f): same as (a) and (b) with 49 stations with minimum inter-site distance of 60 km (274 and  
 1112 214 years in total). Blue curves: median and percentiles 2.5 and 97.5 of the predicted distributions;  
 1113 Red stars: observations. Black stars: reduced number of sites in case of double counting (see the text).

1114





1115

1116 **Figure 14:** (a) Magnitudes of earthquakes producing ground-motion exceedances at the Turkish sites  
1117 (results in Figs. 13a and 13b, considering 189 stations); (b) Joyner and Boore source-site distances of  
1118 the events producing ground-motion exceedances. All events producing the threshold exceedance are  
1119 reported, thus the same event can be reported for different thresholds.

1120

1121

1122

1123 **Appendix A: Input parameters for applying Akkar and Çağnan (2010) GMPE**

1124

1125 The ground-motion prediction equation developed by Akkar and Çağnan (2010) is used to  
1126 predict accelerations at the sites. The earthquake catalogue used is a combination of the  
1127 catalogue used in SHARE and of the KOERI catalogue for the most recent period ( $M_w \geq 4.0$ ).  
1128 The GMPE has been developed from Turkish data, using earthquakes with magnitudes  $M_w$   
1129 3.5 to 7.6. Predictions are performed considering the  $V_{S30}$  values of the sites. To apply the  
1130 equation, the magnitude of the earthquake, the style of faulting, and the Joyner and Boore  
1131 source-to-site distance ( $R_{JB}$ ) are required.  $R_{JB}$  is assumed equal to epicentral distance for  
1132 earthquakes with  $M_w$  lower than 5.5. For earthquakes with  $M_w$  higher than 5.5, most  $R_{JB}$   
1133 distances are taken from the RESORCE database (Akkar et al. 2014). If not in RESORCE,  
1134  $R_{JB}$  is estimated from the nodal plane and an estimate of the fault width and length (scaling  
1135 relations, Leonard 2010). For some earthquakes, two nodal planes are possible, then the nodal  
1136 plane is deduced from the location of the earthquake on the faulting map of Turkey (Bozkurt  
1137 2001). If  $M_w$  is not available in RESORCE, following Akkar et al. (2014) a magnitude is  
1138 looked for in international earthquake catalogues (GCMT, ISC, SED-ETH). If the faulting  
1139 style of  $M_w$  higher than 5.5 is not available in RESORCE, the faulting style is determined  
1140 following the same approach as Akkar et al. 2010 (approaches of Frohlich & Apperson 1992,  
1141 Campbell 1997). For all earthquakes with  $M_w$  lower than 5.5, the focal mechanism is  
1142 assumed to be strike-slip (2/3 of the generating dataset of Akkar and Çağnan 2010  
1143 corresponds to strike slip mechanism).

1144

1145

1146

1147

1148  
1149  
1150  
1151  
1152  
1153  
1154**Supplementary Files****Table S1:** List of the 62 rock RAP French stations used in this study.

Station Name	Latitude (°)	Longitude (°)	Original Lifetime (years)	Corrected Lifetime (years)	# of records with PGA $\geq 1$ cm/s <sup>2</sup>	Maximum recorded PGA (cm/s <sup>2</sup> )
ANTF	43.564	7.123	8.6	3.0	2	2.6
ARBF	43.492	5.332	11.7	4.3	1	1.6
CAGN	43.667	7.146	8.1	3.8	6	2.8
ESCA	43.831	7.374	7.8	6.1	3	2.9
IRJO	43.630	5.660	15.6	15.6	1	5.8
IRPV	43.803	5.759	14.1	0.8	2	11.8
IRSE	44.530	6.780	6.7	6.7	1	2.0
MENA	43.784	7.489	12.5	7.9	18	16.1
NBOR	43.690	7.301	10.6	10.6	3	3.8
OCCD	45.319	3.699	8.0	5.4	1	1.0
OCMN	46.328	2.589	5.7	5.7	1	2.4
OCSJ	46.051	2.733	7.9	5.2	2	3.1
OGAG	44.788	6.540	16.1	6.9	2	2.3
OGCH	45.589	5.933	14.1	5.1	3	1.8
OGGM	45.204	6.117	16.6	7.3	1	1.7
OGLE	45.533	6.473	13.6	13.0	1	4.5
OGMA	45.774	5.535	12.3	10.4	7	15.7
OGAN	45.892	6.136	14.4	9.6	1	1.2
OGMO	45.208	6.685	14.8	10.6	8	9.0
OGMU	45.195	5.727	14.5	9.0	4	1.4
OGSI	46.057	6.756	15.4	12.1	18	27.7
OGTB	46.319	6.596	12.5	12.5	5	2.9
OGTI	45.494	6.925	13.5	13.5	17	6.2
PYAD	43.097	-0.428	7.9	6.6	220	100.9
PYAS	43.012	0.797	9.1	9.1	4	2.9
PYAT	43.094	-0.713	7.7	6.7	63	22.6
PYBA	42.474	3.117	9.3	6.0	3	2.4
PYBE	42.819	1.951	7.3	5.9	3	1.6
PYCA	43.024	0.183	7.9	5.6	127	84.6
PYFE	42.814	2.507	10.1	9.3	5	3.3
PYLL	42.453	2.065	7.6	5.3	2	10.1
PYLO	43.097	-0.049	7.4	6.3	20	26.5
PYLS	42.860	-0.008	10.0	8.7	34	40.8
PYOR	42.783	1.507	8.8	8.0	7	2.7
PYPM	42.416	2.439	10.6	7.9	1	6.8
PYP1	43.156	-1.241	6.8	6.8	1	0.93
PYPR	42.614	2.429	7.6	5.4	3	1.9
PYPT	43.009	3.033	9.9	9.9	1	2.1
QUIF	47.910	-3.160	6.2	2.2	1	2.0
SAOF	43.986	7.553	16.3	13.5	12	117.9
SMFF	46.600	-0.130	6.3	6.3	4	2.4
STBO	47.861	7.262	11.1	5.4	10	10.9
STET	44.260	6.929	12.1	9.5	25	6.6
STFL	47.112	6.563	11.3	3.6	5	22.6

STMU	48.584	7.766	9.9	3.6	28	28.1
STRB	47.723	7.341	5.7	3.0	7	8.1
STSM	48.215	7.159	11.6	8.7	4	25.4
BAIF	50.059	4.208	2.8	2.8	0	†
BRGM	43.237	5.438	9.7	9.7	0	†
UBBR	48.358	-4.562	3.5	3.5	0	†
UBNA	47.156	-1.637	2.8	2.8	0	†
UBVA	47.645	-2.746	2.9	2.9	0	†
CALF	43.753	6.922	15.8	12.0	0	†
IRIS	44.190	7.050	6.6	6.6	0	†
OCOL	45.676	3.636	6.0	6.0	0	†
OCOR	45.798	3.028	7.4	6.5	0	†
OCSF	45.034	3.097	4.0	4.0	0	†
OGBB	44.281	5.259	12.2	12.2	0	†
OGCA	43.732	5.672	15.1	6.5	0	†
PYFO	42.968	1.607	10.6	10.6	0	†
PYLI	43.002	1.136	9.3	9.3	0	†
RUSF	43.941	5.484	10.5	5.2	0	†

1155 † maximum recorded PGA is lower than our database minimum threshold (1 cm/s<sup>2</sup>)

1156  
1157  
1158  
1159  
1160

1161 **Table S2: List of 189 Turkish accelerometric stations considered in this study**

1162

Station ID	Latitude (°)	Longitude (°)	V <sub>S30</sub> (m/s)	Observation time window	Original duration T (yrs)	T <sub>COR1</sub> (yrs)	T <sub>COR2</sub> (yrs)	Maximum recorded PGA (cm/s <sup>2</sup> )	# of records with PGA <sub>≥</sub> 50 cm/s <sup>2</sup>	Maximum PGA <sub>ROCK</sub> (cm/s <sup>2</sup> )	# of records with PGA <sub>ROCK</sub> ≥ 50 cm/s <sup>2</sup>
301	30.53	38.78	226	1998.3 2013.1	14.87	14.87	9.19	103.4	1	82.5	1
905	27.27	37.86	369	1986.4 2013.1	26.72	6.97	10.25	113.9	7	91.5	4
1201	40.50	38.90	529	1997.5 2011.7	14.15	14.15	12.64	388.3	2	358.6	2
1206	41.01	39.29	356	2007.7 2012.6	4.99	4.99	4.99	143.9	1	119.4	1
1606	29.12	40.36	301	2003.2 2013.1	9.89	9.89	6.52	169.1	1	139.6	1
1608	29.18	40.41	366	2003.2 2012.3	9.12	9.12	4.70	83.0	1	66.4	1
1609	29.17	40.43	229	2003.3 2013.0	9.75	9.75	6.68	78.9	1	59.9	1
1612	29.72	40.44	197	1999.6 2000.6	1.02	1.02	0.78	106.4	1	88.3	1
2002	29.11	37.81	356	1994.3 2012.4	18.17	18.17	13.94	165.4	2	136.5	1
2007	28.92	37.93	233	2003.3 2012.5	9.25	6.18	5.18	114.5	3	90.9	2
3102	36.16	36.21	470	1981.5 2006.1	24.64	11.68	11.27	143.1	2	122.9	2
3506	27.08	38.39	771	1977.9 2013.1	35.20	5.69	5.69	221.1	2	223.7	2
1101	29.98	40.14	901	2006.8 2011.5	4.74	4.74	4.74	87.4	1	96.2	1
4106	29.45	40.79	701	1999.6 2013.0	13.39	13.39	5.13	183.4	1	182.6	1
4107	29.93	40.76	305	1999.7 2013.0	13.32	2.65	2.65	448.7	1	444.1	1
4113	29.73	40.78	300	2010.4 2013.0	2.58	2.58	2.58	97.9	1	76.8	1
4304	29.40	38.99	343	2006.8 2012.8	6.02	6.02	3.71	98.1	3	76.9	1
4305	28.98	39.09	259	2006.8 2012.8	6.01	6.01	2.78	196.2	5	170.5	4

4306	29.25	39.34	304	2010.6	2012.8	2.22	2.22	2.20	73.7	1	56.4	1
4504	28.65	39.04	336	2006.8	2013.0	6.22	6.22	6.22	288.2	3	261.2	2
4604	36.36	37.57	611	1997.1	2012.6	15.50	15.50	15.15	265.2	2	253.9	2
4803	29.12	36.63	248	2007.5	2012.5	4.97	4.97	3.97	177.0	1	154.9	1
302	30.15	38.06	198	1995.7	2013.1	17.40	17.40	5.33	295.4	12	318.5	9
4804	28.69	36.97	372	1985.9	2008.5	22.60	22.60	11.71	108.3	2	86.0	2
5401	30.38	40.74	412	1994.5	2012.5	18.06	18.06	18.04	261.8	6	228.5	5
5402	30.62	40.67	272	2000.6	2009.3	8.73	8.73	5.51	87.4	1	67.2	1
6501	43.40	38.50	363	1995.1	2013.2	18.06	18.06	4.64	187.0	1	159.6	1
6503	43.77	38.99	293	1997.8	2012.3	14.51	14.51	1.52	174.0	2	144.6	1
1607	29.10	40.39	176	2003.2	2012.9	9.68	9.68	7.88	190.1	2	190.9	1
8101	31.15	40.84	282	1999.6	2007.1	7.47	7.47	6.12	455.6	2	466.1	2
1801	32.88	40.81	348	1977.8	2006.5	28.76	6.37	6.36	62.8	1	48.9	0
3401	29.01	41.06	595	1995.1	2010.8	15.65	15.65	15.54	50.8	1	47.3	0
502	35.85	40.67	443	1995.9	2006.9	10.99	10.99	10.99	57.8	1	46.7	0
2301	39.19	38.67	407	1995.0	2011.5	16.52	16.52	14.82	55.0	1	44.7	0
4902	42.53	39.14	311	1997.8	2012.2	14.40	14.40	1.18	55.9	1	42.1	0
907	28.47	37.91	301	2003.6	2012.5	8.92	8.92	4.15	54.8	1	40.9	0
4302	30.00	39.42	243	1998.2	2007.7	9.54	9.54	8.92	54.7	1	39.4	0
3502	27.23	38.46	270	1995.8	2007.9	12.10	12.10	12.03	54.0	1	39.4	0
1601	29.08	40.23	249	2003.3	2013.0	9.75	9.75	9.75	53.5	1	38.6	0
1006	28.00	40.33	321	2000.6	2013.0	12.38	12.38	4.90	50.4	1	37.3	0
3409	28.76	41.03	283	2010.8	2012.8	2.04	2.04	2.04	50.3	1	36.1	0
6512	43.76	38.99	293	2012.3	2013.1	0.74	0.74	0.32	†	0	†	0
4906	42.53	39.14	311	2012.5	2012.7	0.25	0.25	0.25	†	0	†	0
1007	27.94	40.34	417	2003.3	2003.5	0.24	0.24	0.24	†	0	†	0
2902	39.44	40.12	612	2011.7	2012.1	0.35	0.35	0.35	†	0	†	0
402	44.09	39.55	271	2006.0	2007.0	0.97	0.97	0.34	†	0	†	0
3801	35.50	38.69	407	2008.9	2009.0	0.17	0.17	0.17	†	0	†	0
902	27.80	37.85	271	2003.7	2004.0	0.28	0.28	0.28	†	0	†	0
5801	38.11	40.17	413	2011.7	2012.0	0.31	0.31	0.31	†	0	†	0
6004	37.33	40.39	376	2012.5	2013.0	0.50	0.50	0.50	†	0	†	0
1001	27.86	39.65	662	1997.7	2008.5	10.76	10.76	9.72	†	0	†	0
4802	27.44	37.03	747	1999.2	2008.5	9.37	9.37	9.31	†	0	†	0
1701	26.40	40.14	192	1997.4	2013.0	15.61	15.61	15.61	†	0	†	0
2501	41.26	39.90	375	1994.9	2009.1	14.19	14.19	12.73	†	0	†	0
1613	29.23	39.92	401	2006.8	2013.1	6.34	6.34	6.34	†	0	†	0
2401	39.51	39.74	314	1993.1	2011.9	18.88	18.88	13.32	†	0	†	0
1502	30.22	37.70	294	1998.2	2012.4	14.29	14.29	13.80	†	0	†	0
4401	38.34	38.35	481	1994.5	2013.0	18.52	18.52	18.50	†	0	†	0
5902	27.52	40.98	409	1994.5	2012.6	18.03	13.03	18.03	†	0	†	0
3510	27.04	38.41	313	2010.6	2013.1	2.56	2.56	2.54	†	0	†	0
3701	34.04	41.01	362	1999.4	2011.6	12.21	12.21	11.78	†	0	†	0
901	27.84	37.84	311	1998.2	2002.1	3.87	3.87	3.87	†	0	†	0
1009	28.63	39.58	561	2006.8	2013.0	6.22	6.22	6.22	†	0	†	0
4810	28.24	36.84	393	2011.3	2013.0	1.78	1.78	1.73	†	0	†	0

3503	26.89	39.07	193	2006.8	2013.0	6.22	6.22	6.15	†	0	†	0
1604	29.13	40.18	457	1997.8	2001.5	3.68	3.68	3.67	†	0	†	0
3516	26.89	38.37	460	2010.8	2013.1	2.30	2.30	2.28	†	0	†	0
3524	27.11	38.50	459	2010.9	2013.1	2.28	2.28	2.26	†	0	†	0
3511	27.26	38.42	827	2010.8	2013.1	2.30	2.30	2.30	†	0	†	0
2603	30.45	39.88	629	2006.9	2012.5	5.58	5.58	5.58	†	0	†	0
6401	29.40	38.67	285	1998.2	2012.5	14.32	14.32	13.80	†	0	†	0
3530	27.22	38.45	270	2010.3	2013.1	2.81	2.81	2.79	†	0	†	0
3523	26.77	38.33	414	2010.8	2013.1	2.30	2.30	2.28	†	0	†	0
4811	28.69	36.97	372	2012.3	2013.1	0.87	0.87	0.87	†	0	†	0
4901	41.50	38.76	315	1994.7	2012.2	17.53	17.53	6.42	†	0	†	0
3521	27.08	38.47	145	2010.9	2013.1	2.28	2.28	2.26	†	0	†	0
3520	27.21	38.48	875	2010.8	2013.0	2.20	2.20	2.20	†	0	†	0
3519	27.11	38.45	131	2010.8	2013.1	2.29	2.29	2.27	†	0	†	0
3514	27.16	38.48	836	2010.8	2013.1	2.29	2.29	2.29	†	0	†	0
3525	27.11	38.37	745	2010.8	2013.1	2.30	2.30	2.30	†	0	†	0
4501	27.38	38.61	340	1998.2	2011.4	13.21	13.21	12.03	†	0	†	0
104	35.81	37.02	223	1998.5	2011.5	13.00	13.00	3.68	†	0	†	0
1003	27.86	39.65	456	2006.8	2013.0	6.19	6.19	3.35	†	0	†	0
603	33.12	39.56	450	2008.2	2011.7	3.48	3.48	3.19	†	0	†	0
1014	27.64	40.11	397	1983.5	2013.0	29.51	6.22	3.46	†	0	†	0
3515	27.09	38.46	171	2010.8	2013.1	2.29	2.29	2.22	†	0	†	0
1208	41.05	38.97	485	1997.7	2007.2	9.45	9.45	5.90	†	0	†	0
2602	30.50	39.79	326	2006.8	2012.9	6.07	6.07	3.66	†	0	†	0
201	38.27	37.76	391	2008.0	2013.0	5.03	5.03	5.03	†	0	†	0
4606	37.14	37.39	484	2004.5	2012.9	8.35	8.35	8.16	†	0	†	0
3512	27.15	38.40	468	2011.0	2013.1	2.16	2.16	2.16	†	0	†	0
3522	27.20	38.44	249	2010.8	2013.1	2.29	2.29	2.22	†	0	†	0
3513	27.17	38.46	196	2010.8	2013.0	2.20	2.20	2.13	†	0	†	0
2606	30.50	39.75	346	2010.6	2012.9	2.26	2.26	2.26	†	0	†	0
3518	27.14	38.43	298	2010.8	2013.0	2.21	2.21	2.10	†	0	†	0
4505	28.28	38.94	629	2012.3	2012.8	0.52	0.52	0.52	†	0	†	0
2406	40.38	39.78	417	2003.3	2006.9	3.56	3.56	3.53	†	0	†	0
6001	36.56	40.33	324	1999.4	2013.2	13.80	13.80	13.80	†	0	†	0
4506	28.12	38.48	273	2007.9	2012.6	4.75	4.75	4.75	†	0	†	0
904	28.05	37.86	367	2003.3	2007.3	4.04	4.04	3.79	†	0	†	0
908	28.34	37.91	267	2003.3	2008.0	4.75	4.75	4.75	†	0	†	0
4301	29.99	39.43	267	2006.8	2012.3	5.53	5.53	5.53	†	0	†	0
909	28.15	37.88	355	2003.3	2012.6	9.32	9.32	9.06	†	0	†	0
1615	29.29	40.42	349	2003.2	2011.4	8.17	8.17	8.17	†	0	†	0
8002	36.56	37.19	430	2010.9	2012.9	2.07	2.07	2.07	†	0	†	0
4111	29.59	40.68	300	2010.4	2013.0	2.65	2.65	2.65	†	0	†	0
4105	29.97	40.67	289	2008.2	2012.5	4.32	4.32	4.32	†	0	†	0
2601	30.53	39.81	231	2006.8	2011.5	4.73	4.73	3.51	†	0	†	0
2404	38.77	39.91	413	2011.7	2012.9	1.22	1.22	1.22	†	0	†	0
4801	28.36	37.21	468	2007.8	2012.7	4.84	4.84	2.76	†	0	†	0

309	31.24	38.53	387	2007.3	2012.5	5.22	5.22	5.22	†	0	†	0
910	27.80	37.85	271	2010.8	2012.5	1.76	1.76	1.76	†	0	†	0
4603	36.93	37.58	466	1995.3	2004.2	8.92	8.92	8.92	†	0	†	0
1005	26.69	39.31	387	2006.8	2013.0	6.22	6.22	6.22	†	0	†	0
4112	29.84	40.72	352	2010.4	2013.0	2.65	2.65	2.65	†	0	†	0
208	37.65	37.79	469	2011.2	2013.0	1.78	1.78	1.78	†	0	†	0
2701	36.64	37.03	421	1994.0	2012.7	18.71	18.71	7.27	†	0	†	0
4502	27.82	38.91	292	2007.6	2012.9	5.30	5.30	1.23	†	0	†	0
2405	40.39	39.78	320	1992.2	2003.1	10.87	10.87	5.87	†	0	†	0
4608	36.84	37.38	390	2006.3	2012.9	6.56	6.56	6.56	†	0	†	0
2607	30.15	39.82	274	2006.8	2011.4	4.58	4.58	4.58	†	0	†	0
1616	29.26	40.45	572	2004.4	2011.4	7.01	7.01	5.10	†	0	†	0
1603	29.13	40.18	457	2006.8	2013.0	6.22	6.22	6.22	†	0	†	0
4605	37.20	38.20	315	1996.9	2001.5	4.63	4.63	4.63	†	0	†	0
2307	39.93	38.70	329	2011.4	2013.1	1.72	1.72	1.72	†	0	†	0
2604	30.51	39.77	296	2006.8	2012.3	5.54	5.54	1.04	†	0	†	0
5904	27.12	40.61	225	2012.2	2013.0	0.83	0.83	0.83	†	0	†	0
4607	37.30	37.49	671	2006.3	2012.9	6.60	6.60	6.60	†	0	†	0
4403	37.89	38.10	654	1996.8	2007.0	10.15	10.15	10.15	†	0	†	0
3105	36.51	36.80	618	2004.6	2012.9	8.28	8.28	8.28	†	0	†	0
1301	42.28	38.50	273	1997.4	2011.8	14.39	14.39	2.02	†	0	†	0
3109	36.41	36.58	272	2004.6	2012.9	8.28	8.28	3.09	†	0	†	0
1904	34.94	40.55	193	2008.8	2012.9	4.11	4.11	2.63	†	0	†	0
4104	29.97	40.68	757	2010.7	2012.5	1.77	1.77	1.77	†	0	†	0
4110	30.15	41.07	380	2010.4	2012.5	2.14	2.14	2.14	†	0	†	0
1614	28.39	40.03	265	2006.8	2012.3	5.54	5.54	5.54	†	0	†	0
1610	29.51	40.07	252	2012.3	2013.0	0.73	0.73	0.73	†	0	†	0
1013	27.02	39.59	223	1983.5	2013.0	29.51	29.51	5.17	†	0	†	0
6301	38.80	37.17	652	2008.5	2010.7	2.20	2.20	2.20	†	0	†	0
4601	36.98	37.54	346	2004.5	2012.9	8.41	8.41	5.00	†	0	†	0
703	30.15	36.30	299	2000.8	2012.4	11.63	11.63	11.63	†	0	†	0
604	33.52	38.96	291	2008.2	2011.4	3.20	3.20	3.20	†	0	†	0
2703	37.35	37.06	758	2008.7	2012.8	4.12	4.12	4.12	†	0	†	0
3104	36.49	36.69	688	2004.6	2012.9	8.28	8.28	8.28	†	0	†	0
3101	36.16	36.21	470	2006.1	2013.1	6.97	6.97	2.35	†	0	†	0
4102	30.03	40.78	1013	2010.7	2013.0	2.27	2.27	2.27	†	0	†	0
2702	36.73	37.18	599	2007.6	2013.1	5.47	5.47	4.91	†	0	†	0
1102	30.05	39.90	407	2006.8	2011.5	4.73	4.73	4.73	†	0	†	0
7701	29.31	40.56	375	2004.4	2013.0	8.65	8.65	8.65	†	0	†	0
4701	40.72	37.33	709	2008.7	2012.6	3.93	3.93	3.93	†	0	†	0
1605	29.10	40.27	495	2003.2	2012.5	9.25	9.25	5.72	†	0	†	0
3111	36.22	36.37	338	2005.6	2012.7	7.15	7.15	2.77	†	0	†	0
3107	36.18	36.58	310	2004.5	2012.7	8.18	8.18	1.53	†	0	†	0
7801	32.62	41.20	703	2000.1	2001.7	1.53	1.53	1.53	†	0	†	0
1211	41.05	38.97	463	2011.8	2012.7	0.93	0.93	0.93	†	0	†	0
7702	29.27	40.59	359	2004.8	2011.4	6.61	6.61	4.90	†	0	†	0

8001	36.27	37.08	350	2005.1	2012.9	7.86	7.86	1.31	†	0	†	0
1703	27.26	40.23	304	2012.3	2013.0	0.74	0.74	0.74	†	0	†	0
1710	26.67	40.42	286	2012.4	2013.0	0.64	0.64	0.64	†	0	†	0
2302	39.68	38.39	907	2011.5	2012.7	1.19	1.19	1.19	†	0	†	0
1017	27.86	39.65	662	2012.2	2013.0	0.83	0.83	0.83	†	0	†	0
7201	41.15	37.87	450	2010.2	2012.5	2.27	2.27	2.27	†	0	†	0
1505	29.78	37.32	367	2012.4	2013.0	0.57	0.57	0.57	†	0	†	0
1611	29.72	40.43	251	2004.4	2013.0	8.65	8.65	0.68	†	0	†	0
1617	29.30	40.49	1598	2004.4	2013.0	8.65	8.65	1.99	†	0	†	0
4404	38.52	38.12	1380	2011.5	2012.4	0.92	0.92	0.92	†	0	†	0
2901	39.50	40.45	469	2010.2	2011.6	1.40	1.40	1.40	†	0	†	0
3501	27.17	38.46	196	1992.8	1995.1	2.24	2.24	0.69	†	0	†	0
4103	30.03	40.79	1013	2008.2	2012.5	4.32	4.32	4.32	†	0	†	0
3408	28.26	41.07	639	2010.8	2013.0	2.26	2.26	1.03	†	0	†	0
2608	31.18	39.52	476	2008.0	2011.4	3.42	3.42	3.42	†	0	†	0
2507	42.17	40.04	316	2012.0	2013.1	1.10	1.10	1.10	†	0	†	0
506	35.80	40.64	284	2010.8	2013.2	2.41	2.41	2.41	†	0	†	0
118	35.19	37.02	946	2008.0	2011.5	3.46	3.46	3.46	†	0	†	0
3108	36.37	36.50	539	2008.3	2012.9	4.53	4.53	4.53	†	0	†	0
3103	36.25	36.12	344	2006.1	2008.3	2.20	2.20	2.20	†	0	†	0
401	43.02	39.72	295	2007.1	2011.8	4.76	4.76	4.76	†	0	†	0
1903	34.80	40.98	255	2011.7	2012.2	0.52	0.52	0.52	†	0	†	0
7704	29.25	40.66	195	2008.2	2013.0	4.82	4.82	1.97	†	0	†	0
4001	34.16	39.16	460	2008.7	2012.8	4.03	4.03	4.03	†	0	†	0
3110	35.95	36.08	210	2004.3	2008.3	3.99	3.99	3.99	†	0	†	0
6005	36.57	40.70	327	2010.9	2013.2	2.32	2.32	2.32	†	0	†	0
7703	29.28	40.65	278	2010.4	2012.3	1.90	1.90	1.90	†	0	†	0
2101	40.20	37.93	519	2010.2	2010.7	0.53	0.53	0.53	†	0	†	0
6901	40.21	40.26	519	2011.0	2011.8	0.82	0.82	0.82	†	0	†	0
801	41.84	41.18	350	2011.1	2013.0	1.94	1.94	1.94	†	0	†	0
3601	43.08	40.60	270	1995.8	1997.8	2.10	2.10	2.10	†	0	†	0
7601	44.05	39.93	216	1998.1	1998.7	0.67	0.67	0.67	†	0	†	0
6801	34.03	38.35	208	2008.9	2011.5	2.59	2.59	2.59	†	0	†	0

- 1163 T: time elapsed between the 1<sup>st</sup> and the last record available at the station  
 1164 T<sub>COR1</sub>: corrected observation time window, gaps identified using method 1 (inter-event times)  
 1165 T<sub>COR2</sub>: corrected observation time window, gaps identified using method 2 (synthetic accelerations)  
 1166 PGA: recorded PGA at the site (176 soil sites, 13 rock sites)  
 1167 PGA<sub>ROCK</sub>: estimated PGA at V<sub>S30</sub>=750m/s, inferred from the recorded PGA and the site-amplification model of Sandikkaya  
 et al. (2013)  
 1169 † maximum recorded PGA is lower than our database minimum threshold (50 cm/s<sup>2</sup>)  
 1170  
 1171  
 1172  
 1173  
 1174  
 1175  
 1176  
 1177  
 1178



1179 **Table S3: 56 observations with  $PGA_{750} \geq 50$  cm/s/s recorded at the stations of the Turkish**  
 1180 **network and used in the testing**

Record ID (yyyymmddhhmmss)	$M_w$	Lat (°)	Long (°)	Depth (km)	Style of Faulting	Station ID	$R_{JB}$ (km)	$PGA_{ROCK}$ (cm/s/s)	PGA (cm/s/s)
19771209155338	5.1	38.35	27.23	26.9	Strike-Slip	3506	13.4	115.5	114.2
19771216073729	5.6	38.39	27.19	4.0	Normal	3506	6.0	223.7	221.1
19810630075909	4.7	36.17	35.89	63.0	Normal	3102	25.0	111.4	130.4
19851206223530	5.1	36.97	28.85	8.9	Strike-Slip	4804	14.7	86.8	108.3
19860601064310	4.2	37.96	27.39	10.0	Strike-Slip	0905	15.5	50.4	64.7
19921106190809	6.0	38.09	27.05	15.0	Strike-Slip	0905	40.0	59.3	75.7
19941113065601	5.3	36.91	29.05	10.0	Normal	4804	30.0	64.0	81.2
19950314000651	4.1	37.88	29.07	5.0	Normal	2002	8.7	136.5	165.4
19950926145809	4.9	38.03	30.17	18.8	Strike-Slip	0302	3.3	119.8	138.0
19950927141554	5.0	38.07	30.20	11.3	Strike-Slip	0302	4.1	102.5	122.0
19951001155713	6.5	38.12	30.11	10.0	Normal	0302	0.0	318.5	295.4
19951001180256	5.3	38.05	30.16	28.4	Strike-Slip	0302	1.7	137.2	153.6
19951001211442	4.4	38.00	30.08	16.8	Strike-Slip	0302	8.9	102.7	122.2
19951003073811	4.9	37.97	30.08	11.0	Strike-Slip	0302	11.9	79.8	99.7
19951005161521	5.0	38.00	30.14	11.8	Strike-Slip	0302	6.7	93.8	113.7
19951006161558	4.8	38.03	30.14	34.5	Strike-Slip	0302	3.6	106.6	125.8
19970122175720	5.7	36.21	35.97	20.0	Normal	3102	19.0	122.9	143.1
19980404161747	5.2	38.1	30.1	19.3	Normal	0302	2.0	112.9	131.7
19990817000139	7.6	40.76	29.96	17.0	Strike-Slip	1612	38.0	88.3	106.4
19990817000139	7.6	40.76	29.96	17.0	Strike-Slip	4106	38.0	182.6	183.4
19990817000139	7.6	40.76	29.96	17.0	Strike-Slip	8101	7.0	322.2	337.4
19990913115529	5.8	40.76	30.05	15.0	Strike-Slip	4107	3.0	444.1	448.7
19991111144127	5.6	40.79	30.22	14.3	Strike-Slip	5401	10.0	228.5	261.8
19991112165721	7.1	40.82	31.20	11.2	Strike-Slip	8101	0.0	466.1	455.6
20000402185742	4.5	40.86	30.29	8.8	Strike-Slip	5401	15.0	62.1	76.8
20000823134129	5.5	40.68	30.72	15.0	Strike-Slip	5402	5.0	67.2	87.4
20020203071129	6.5	38.58	31.16	10.0	Normal	0301	55.0	80.9	103.4
20021214010248	4.8	37.52	36.20	10.0	Normal	4604	13.0	57.3	62.0
20030501002708	6.3	38.95	40.40	15.0	Strike-Slip	1201	10.0	358.6	388.3
20030501093555	4.1	38.87	40.54	9.1	Strike-Slip	1201	5.0	83.0	94.3
20030723045609	5.3	38.05	28.89	28.3	Normal	2007	11.0	82.7	105.7
20030726083654	5.4	38.06	28.91	21.3	Normal	2007	11.0	90.9	114.5
20060208040743	4.5	40.71	30.41	6.8	Normal	5401	3.0	109.6	132.2
20060208052427	4.1	40.71	30.38	4.1	Strike-Slip	5401	3.3	63.1	78.0
20061024140025	5.2	40.42	28.99	7.9	Normal	1609	13.0	59.9	78.9
20061024140026	5.2	40.42	28.99	7.9	Normal	1608	14.0	66.4	83.0
20061024140038	5.2	40.42	28.99	7.9	Normal	1606	11.0	139.6	169.1
20061024140041	5.2	40.42	28.99	7.9	Normal	1607	7.0	190.9	190.1
20070825220536	5.3	39.29	41.03	15.8	Strike-Slip	1206	1.0	119.4	143.9
20090217052819	5.2	39.13	29.05	15.5	Normal	4504	34.0	63.9	82.9
20101111200800	5.0	37.86	27.37	14.0	Normal	0905	8.0	79.3	99.6

20101208215052	3.4	37.83	27.36	13.5	Strike-Slip	0905	9.2	91.5	113.9
20110120020936	4.2	40.73	29.77	12.5	Strike-Slip	4113	5.0	76.8	97.9
20110519201522	5.9	39.14	29.08	12.0	Normal	4304	26.0	76.9	98.1
20110519201522	5.9	39.14	29.08	12.0	Normal	4306	23.0	56.4	73.7
20110519201522	5.9	39.14	29.08	12.0	Normal	4504	33.0	261.2	288.2
20110524025528	3.7	39.10	28.96	5.0	Strike-Slip	4305	2.0	63.5	84.7
20110528054717	5.1	39.12	29.05	9.2	Normal	4305	5.0	75.0	98.0
20110627211358	5.0	39.11	29.03	10.4	Normal	4305	3.0	80.1	103.7
20110711160912	4.5	40.25	29.95	5.0	Normal	1101	11.0	96.2	87.4
20111023104120	7.1	38.75	43.46	16.0	Reverse	6503	0.0	144.6	174.0
20111109192333	5.6	38.43	43.23	8.0	Strike-Slip	6501	15.0	159.6	187.0
20120503152025	5.3	39.18	29.09	3.1	Normal	4305	11.0	170.5	196.2
20120610124415	6.1	36.34	28.67	40.0	Strike-Slip	4803	47.0	154.9	177.0
20120707070745	4.2	40.82	30.41	6.6	Strike-Slip	5401	9.6	53.3	66.3
20120722092602	4.8	37.55	36.38	7.6	Normal	4604	2.0	253.9	265.2

1181 Lat and Lon : Latitude and longitude of the earthquake  
 1182 Depth: Depth of the earthquake in kilometres.  
 1183  $R_{JB}$  distances are mainly from RESORCE database  
 1184 PGA: recorded PGA at the site (176 soil sites, 13 rock sites)  
 1185  $PGA_{ROCK}$ : estimated PGA at  $V_{S30}=750\text{m/s}$ , inferred from the recorded PGA and the site-amplification model of Sandikkaya  
 1186 et al. (2013)  
 1187  
 1188  
 1189  
 1190  
 1191  
 1192  
 1193  
 1194